Electronic Supplementary Material (ESI) for Dalton Transactions.
This journal is © The Royal Society of Chemistry 2021

SUPPORTING INFORMATION

Dual sensing of methionine and aspartic acid in aqueous medium by quinoline based fluorescent probe

C. Elamathi,[a] R.J. Butcher,[b] A. Mohankumar,[c] P. Sundararaj,[c] K. P. Elango[d], P. Kalaivani[e], and R. Prabhakaran*[a]

[a]Department of Chemistry, Bharathiar University, Coimbatore- 641 046, India

[b]Department of Inorganic and Structural Chemistry, Howard University, Washington DC 20059.

[c]Department of Zoology, Bharathiar University, Coimbatore 641 046, India

[d]Department of Chemistry, Gandhigram Rural Institute (Deemed to be University), Gandhigram 624 302, India.

[e]Department of Chemistry, Nirmala College for Women, Red Fields, Coimbatore-641018, India.

Experimental section

Materials and methods

6-methyl-2-oxo-1,2-dihydro-quinoline-3carboxaldehyde was synthesized according to the literature procedure.[1]The other organic chemicals and inorganic salts were purchased from commercial sources and used without further purification. Infrared spectra were taken on a Jasco FT-IR 400-4000 cm^{-1} range using KBr pellets. Electronic spectra were recorded on a JASCO 600 spectrophotometer and fluorescence property was measured using a Jasco FP-6600 spectrofluorometer at room temperature (298 K). ^1H NMR, spectra were recorded in DMSO-d^6 at room temperature with a Bruker 400 MHz instrument, chemical shift relative to tetramethylsilane. The chemical shifts are expressed in parts per million (ppm). High resolution mass spectra were recorded on a Bruker mass spectrometer. Single crystal data collections and corrections for the **6MPS**, **6MPSC** and **6MPSCN** were done at 293 K with CCD Kappa Diffractometer using graphite monochromated Mo Ka (k = 0.71073 A) radiation.[2] The structural solution were done by using SHELXS-97 and refined by full matrix least square on F^2using SHELXL-2014.[3]

Synthesis of 6-Methyl-2-oxo-1,2-dihydroquinoline-3-carboxaldehyde-4(N)-phenylsemicarbazone (6MPS)

6-Methyl-2-oxo-1,2-dihydroquinoline-3-carboxaldehyde (1 g, 5 mmol) in 25 cm^3 of methanol was taken in a Schlenk flask and was degassed with continuous flow of nitrogen. To this methanolic solution of 4-phenylsemicarbazide (0.997 g, 5 mmol) was added by dropwise. Finally, the mixture was degassed again with nitrogen and was refluxed with constant stirring. A yellow precipitate was formed immediately and was further refluxed with stirring about 30 minutes. The formed product was filtered and recrystallized with DMF/MeOH mixture which afforded suitable crystals for X-ray diffraction studies.Yield: 87 %, Mp: 285 ˚C. FT-IR (KBr disks, cm^{-1}): 1655($\upsilon_{C=O}$) (oxo); 1592($\upsilon_{C=N}$); 1679($\upsilon_{C=O}$) (ketoamide). UV-vis (ethanol: water (1:5)), λ_{max}: 288 (12,034) nm (dm^3 $mol^{-1}cm^{-1}$) (л→л*); 331 (12,878), 367 (12,214) (dm^3 $mol^{-1}cm^{-1}$) nm (n→л* transition); ^1H NMR (DMSO-d^6, ppm): 11.92 (s, 1H, N(3)H), 10.92 (s, 1H, N(1)H), 8.94 (s, 1H, N(4)H), 8.70 (s, 1H, -CH=N), 8.21 (s, 1H, C(4)H), δ 7.53 (s, 1H, C(5)H), δ 7.674-7.676 (d, 1H, C(7)H), δ 7.695-7.697 (d, 1H, C(8)H), δ 7.355-7.380 (d, 1H, C(2)H for terminal phenyl), δ 7.239-7.260 (d, 1H, C(6)H for terminal

phenyl), δ 7.303-7.343 (t, 1H, C(3)H for terminal phenyl), δ 7.027-7.064 (t, 1H, C(4)H for terminal phenyl), 2.37 (s, 3H, -CH_3, C(6)).

Preparation of stock solutions for cationic colorimetric titrations

Stock solution of **6MPS** was prepared (20 mM in ethanol: water (1:5)) at pH = 7.2. The solutions of the guest cation using their chloride salts in the concentration of 10 μM and similar concentration for nitrate salts were prepared in aqueous solution. Solutions of various concentrations containing host and increasing concentrations of cations were prepared separately. The spectra of these solutions were recorded by means of absorbance as well as fluorescence methods. Where Cu^{2+} was added gradually to **6MPS** and fluorescence spectra were recorded. For fluorescence study, excitation wavelength used was 391 nm (excitation slit = 5.0 nm and emission slit = 5.0 nm). A series of solutions containing **6MPS** (10 μM in ethanol: water (1:5)) and copper ions (chloride and nitrate) (10 μM) in aqueous solution were prepared in such a manner that the sum of the volume of total metal ion and (**6MPSC** and **6MPSCN)** remained constant (4 mL) at pH 7.2. Job's plots were drawn by plotting ΔF versus mole fraction of Cu^{2+} (chloride). A similar method was followed to prepare the solutions of Job's plot for **6MPS** and Cu^{2+} (nitrate).[4]

A similar procedure was adopted by preparing the stock solutions for fluorescent probe, and different L-amino acids such as arginine (arg), alanine (ala), valine (val), asparagine (aspara), leucine (leu), aspartic acid (asp), glutamic acid (glu), histidine (his), phenylalanine (phenylala), proline (pro), threonine (thr) and methionine (met) (10 μM) which were added to the solutions of **6MPSC** and **6MPSCN** (10 μM). The spectra of these solutions were recorded both absorbance and fluorescence methods. Where methionine and aspartic acid were added gradually to both the solutions (**6MPSC** and **6MPSCN**), emission intensity increased gradually. For fluorescence study, excitation wavelength used was 382 nm (excitation slit = 5.0 nm and emission slit = 5.0 nm). A series of solutions containing **6MPSC** and **6MPSCN** (10 μM) and methionine/aspartic acid (10 μM) were prepared in such a manner that the sum of the total volume of (**6MPS**C and **6MPSCN**) and methionine/ aspartic acid remained constant (4 mL) in aqueous solution at pH 7.2. Job's plots were drawn by plotting ΔF versus mole fraction of methionine/aspartic acid. A similar method was followed to prepare the solutions of Job's plot for **6MPSCN** and methionine/ aspartic acid.[5]

MCF-7 live cell bio-imaging

MCF-7 cells were seeded on cover slips in six well plates for overnight with RPMI media and 10% FBS. On the next day cells were treated with **6MPS** (10 μM in ethanol: water (1:5)), Cu^{2+} ((chloride and nitrate) 10 μM in aqueous solution**)** and methionine/ aspartic acid (10 μM in aqueous solution) respectively for 1 h. After treatment, cells were fixed with methanol and washed with 0.5% Phosphate buffer saline Tween (PBST) twice and then with 1×PBS thrice. The cover slips were mounted on slides using glycerol. The slides were observed under fluorescent microscope (LeicaDM4000 B, Germany) under 20X magnification.[6]

C. elegans maintenance and culture conditions

Wild-type N2 C. elegans was obtained from the Caenorhabditis Genetics Center (University of Minnesota, MN, USA) and maintained on to the nematode growth media agar plates spotted with E. coil OP50 (uracil auxotrophs) at 20°C as described previously.[7,8]For age synchronization, eggs were extracted using sodium hydroxide-sodium hypochlorite solution from gravid adult worms and then maintained in M9 medium (6 g Na_2HPO_4, 3 g KH_2PO_4, 5 g NaCl, 0.25 g $MgSO_4.7H_2O$ and 1 L deionized water) at 20°C to favour the hatching.[9]

Feeding, imaging and image analysis

The age-synchronized L4 larvae of wild-type nitrogen worms (n=35-40/experiment) were exposed to PBS buffer solution containing 10 μM **6MPS** in ethanol: water (1:5) for 6 h at 20 °C. After exposure, the worms were washed thrice with PBS buffer. The worms were then exposed to 10 μM copper(II) chloride and copper(II) nitrate in aqueous solution for 4 h at room temperature. For methionine treated samples, previously exposed L4 stage worms were transferred to Eeppendorf tube filled with 1 mL of PBS buffer and 10 μM of methionine/ aspartic acid in aqueous solution at 20 °C for 4 h. At the end of treatment, the worms were collected and washed three time with PBS buffer before being mounted on a 3 % agar padded microscopic slides. The imaging of immobilized live worms were taken using upright fluorescence microscope (BX41, Olympus, Japan) which was equipped with a digital camera (E330, Olympus, Japan). The captured images were analysed for fluorescence signal by determining the mean pixel intensity using image J software and the acquired data was

subjected to one-way analysis of variance (ANOVA) followed by Bonferroni post-hoc test (SPSS 17, IBM Corporation, NY, USA).[5,9]

Results and Discussion

Spectral description of the probe 6MPS

Vibrational spectrum of **6MPS** showed their corresponding functional group bands at 1679 cm^{-1}, 1655 cm^{-1} and 1592 cm^{-1} for keto amide $\nu_{C=O}$,oxo $\nu_{C=O}$, and azomethine $\nu_{C=N}$ groups respectively.[10] Absorption spectrum of **6MPS** (20 mM) recorded in ethanol: water (1:5) mixture showed bands at 288, 331 and 367 nm for transition within the ligand moiety (intra-ligand transitions).[10] Proton NMR spectrum of **6MPS** recorded in DMSO-d^6 (Figure S1) showed various resonance signals. Singlets at δ 11.92, δ 10.92, δ 8.94, δ 8.70 and δ 8.21 ppm have been assigned to N(1)H, N(3)H, N(4)H, C(1)H and C(4)H protons respectively.[11,12] In the spectrum, C(5) proton appeared as singlet at δ 7.53 ppm, C(7) and C(8) protons appeared as doublet at δ 7.674-7.676 ppm and 7.695-7.697 ppm, respectively.[10] Terminal phenyl protons for C(2) and C(6) positions appeared as a doublet at δ 7.355-7.380 ppm and δ 7.239-7.260 ppm, respectively.[10] Whereas, C(3) and C(5) protons were mixed together and appeared as a triplet at δ 7.303-7.343.[11] Triplet at δ 7.027-7.064 ppm for C(4) proton and a singlet at δ 2.37 ppm owing to methyl protons in quinoline ring were also observed.[12]

The stoichiometric binding between **6MPSC** and **6MPSCN** with methionine and aspartic acid has been confirmed by the spectroscopic studies such as IR, NMR, EPR and mass spectroscopy (Figure S28-S42). From the IR spectra of **6MPSC** and **6MPSCN**, it is clearly inferred that **6MPS** bonded with copper metal ion through quinoline oxygen, azomethine nitrogen and amide oxygen atom of semicarbazone. Further, the binding of amino acids methionine and aspartic acid with of **6MPSC** and **6MPSCN** also confirmed through the asymmetric and symmetric stretching vibrations of carboxylic group. Further, through NMR titration it is clear that **6MPSC, 6MPSCN, 6MPSC-met and 6MPSCN-met, 6MPSC-asp** and **6MPSCN-asp** are NMR absent and EPR confirmed them all are paramagnetic nature. Further, mass spectral analysis and elemental analyses confirmed the 1:1 binding stoichiometry of the complexes.

X-ray crystallographic description of 6MPS and 6MPSCN

The **6MPS** crystallizes in a hexagonal crystal system and space group *p61*(Table S1). The observed bond distance (C(12A)=O(2A), 1.244(18) Å) is comparable with the previously reported literature values. [13] Intermolecular hydrogen bonding played an important role to connecting the three similar units with differ in the bond distances and bond angles (Figure S2, S3). Suitable crystals of **6MPSCN** were obtained from hot methanol: water (1:1) exhibiting ONO pincer type of binding of coordinated **6MPS**. The remaining sites are occupied by oxygen atom of nitrate ion and solvated methanol. Further, a longer Cu-O(8) bond was found with the length of 2.804 Å and notified as not a true bond in which gives a pseudo octahedral geometry around copper ion (Figure S13). The presence of nitrate ion outside the coordination sphere compensated the charge of Cu^{2+}. A water molecule has been found in the crystal lattice which may come through solvent of crystallization. The bond length and bond angles are found to be similar to the reported values (Table S2).[10,14]

Hydrogen bonding description for 6MPSC and 6MPSCN

Further, the intermolecular hydrogen bonding plays a vital role to interconnecting the two different structural units (Figure S14, S15 and Table S3). It is important to note that two different structural units are indicated as **A** and **B** and one complete structure indicated as **#1**. Mainly, hydrogen atom of imine nitrogen N(3B), which is present in second unit **B** bonded to first unit of basal chloride ion Cl(2), N(3B)-H(3BB)···Cl(2). Intermolecular hydrogen bonding formed between second unit of hydrogen atom of terminal nitrogen N(4B) and lattice water molecule N(4B)-H(4BA)···O(2W). Further, hydrogen of lattice water molecule O(2W), which is present in the second unit of lattice bonded to basal chloride ion O(2W)-H(2W2)···Cl(2). Those hydrogen bondings are mainly involves to making the two different structural units (**A** and **B**) by co-crystallization. However, First unit of hydrogen of quinoline nitrogen bonded to second unit of lattice chloride ion Cl(4), N(1A)-H(1AA)···Cl(4). In addition, hydrogen of imine nitrogen N(3A) bonded to first structure (#1) of lattice chloride ion N(3A)-H(3AB)···Cl(4)#1. Terminal nitrogen N(4A), which is present in first unit **B** bonded to first unit of lattice water molecule N(4A)-H(4A)···O(1W)#1. In addition, intermolecular hydrogen bonding formed between oxygen O(3B) atom of methanol in the basal plane and lattice ion of the third unit (#3) O(3B)-H(3B)···Cl(4)#3. However, intermolecular hydrogen bonding formed between hydrogen of quinoline nitrogen N(1A) in the second unit and basal chloride ion in fourth unit

(#4), N(1B)-H(1BA)···Cl(2)#4. Further, hydrogen atoms of lattice water molecules present in both the unit (**A**&**B**) bonded to lattice chloride ion Cl(4) and apical chloride ion in second unit **B,** O(1W)-H(1W1)···Cl(4) and O(2W)-H(2W1)···Cl(3)#1, respectively. Intermolecular hydrogen bonding formed between oxygen O6 atom of hydroxyl group in solvated methanol molecule in axial position and oxygen O7 atom of lattice nitrate molecule O(6)-H(6)···O(7). However, hydrogen atom of lattice water molecule O(1W) bonded to coordinated nitrate molecule in a different manner, like O(3), O(4), N(5) and O(7), O(1W)-H(1W1)···O(3)#1, O(1W)-H(1W1)···O(4)#1, O(1W)-H(1W1)···N(5)#1 and O(1W)-H(1W2)···O(7). Further, hydrogen of quinoline nitrogen intermolecular bonding through lattice water molecule N(1)-H(1A)···O(1W). Hydrogen of imine nitrogen N(3) and terminal nitrogen N(4) bonded to oxygen O(8) and O(9) atoms of lattice nitrate molecule in second structural unit, N(3)-H(3B)···O(8)#2 and N(4)-H(4A)···O(9)#2 respectively. Hydrogen bonding and molecular packing diagrams are shown in Figure S16, 17 and Table S3.

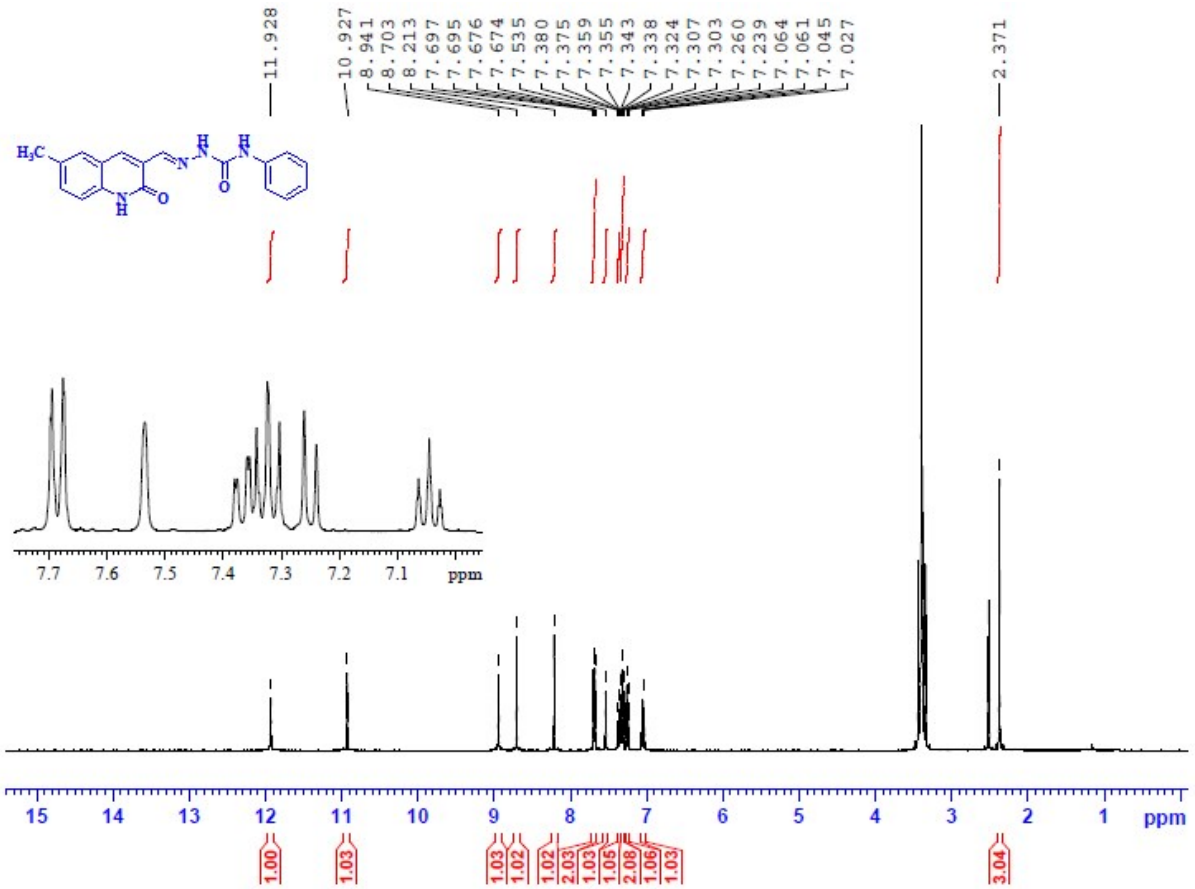

Figure S1 [1]H NMR spectra of**6MPS**.

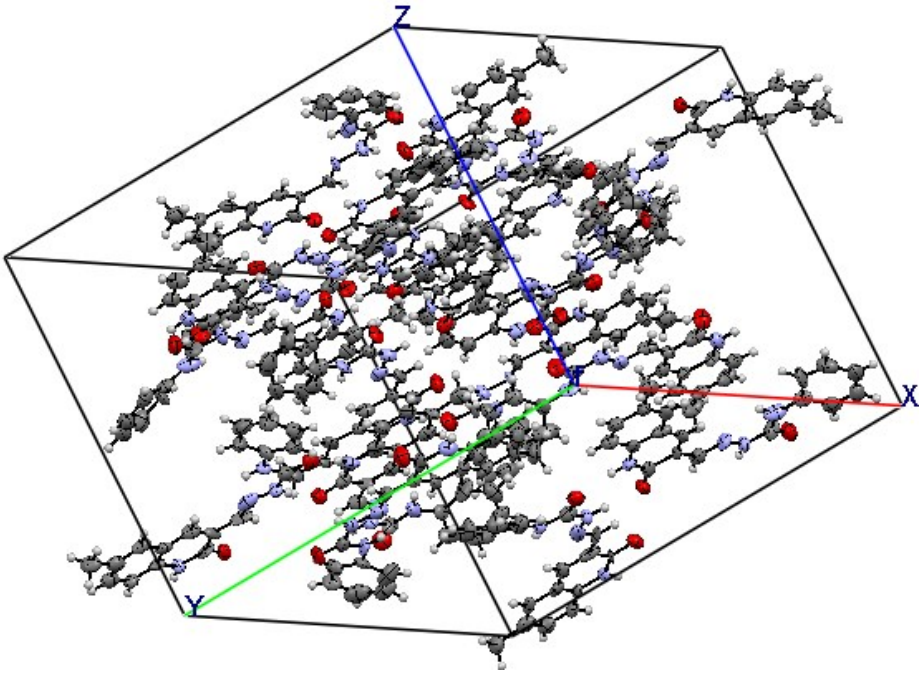

Figure S2 Molecular packing diagram for **6MPS**.

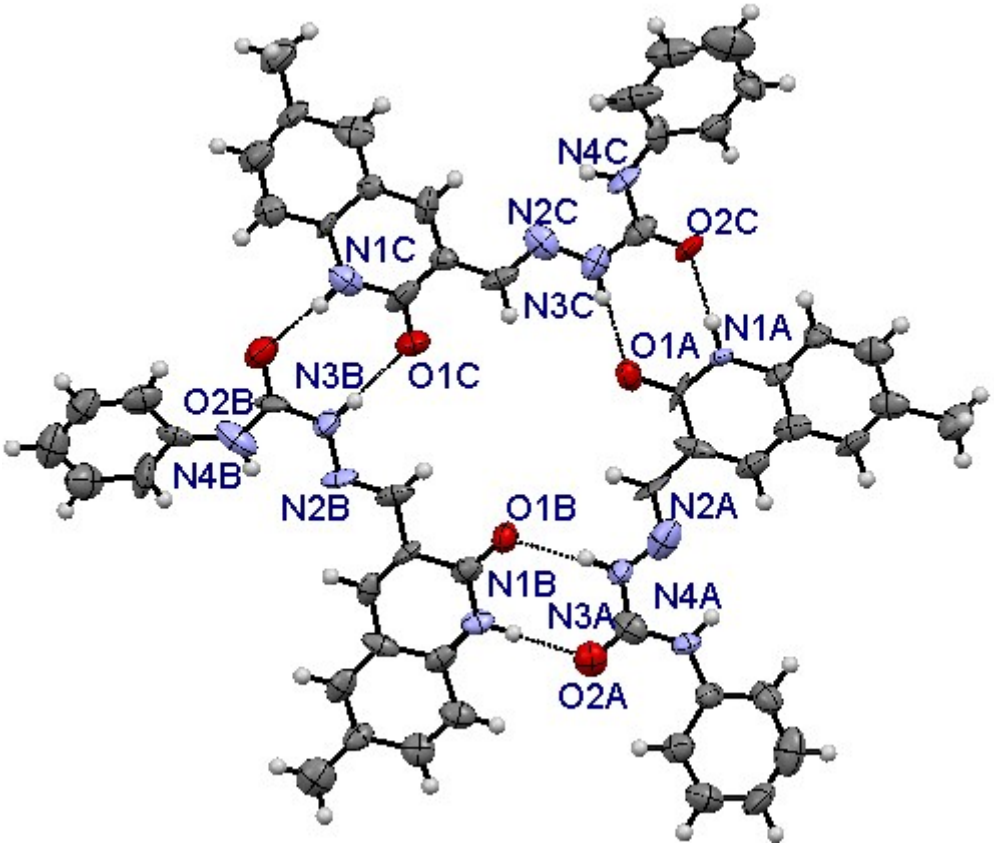

Figure S3 Hydrogen bonding diagram for **6MPS**.

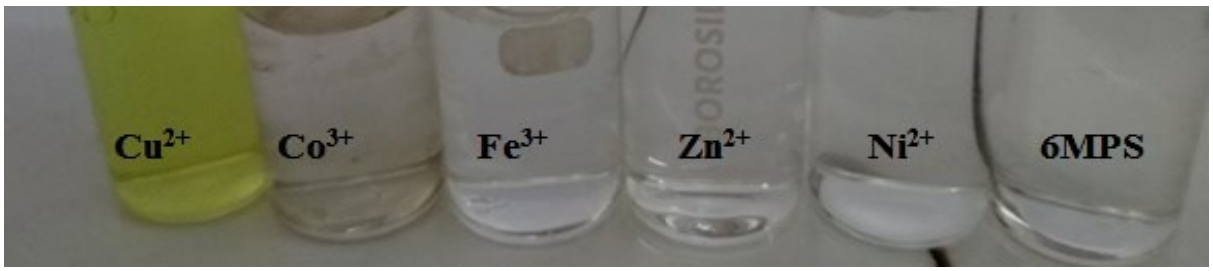

Figure S4 Changes in colour under naked eye, **6MPS** (ethanol: water, 10 μM (1:5)) with nitrate salts of various cations.

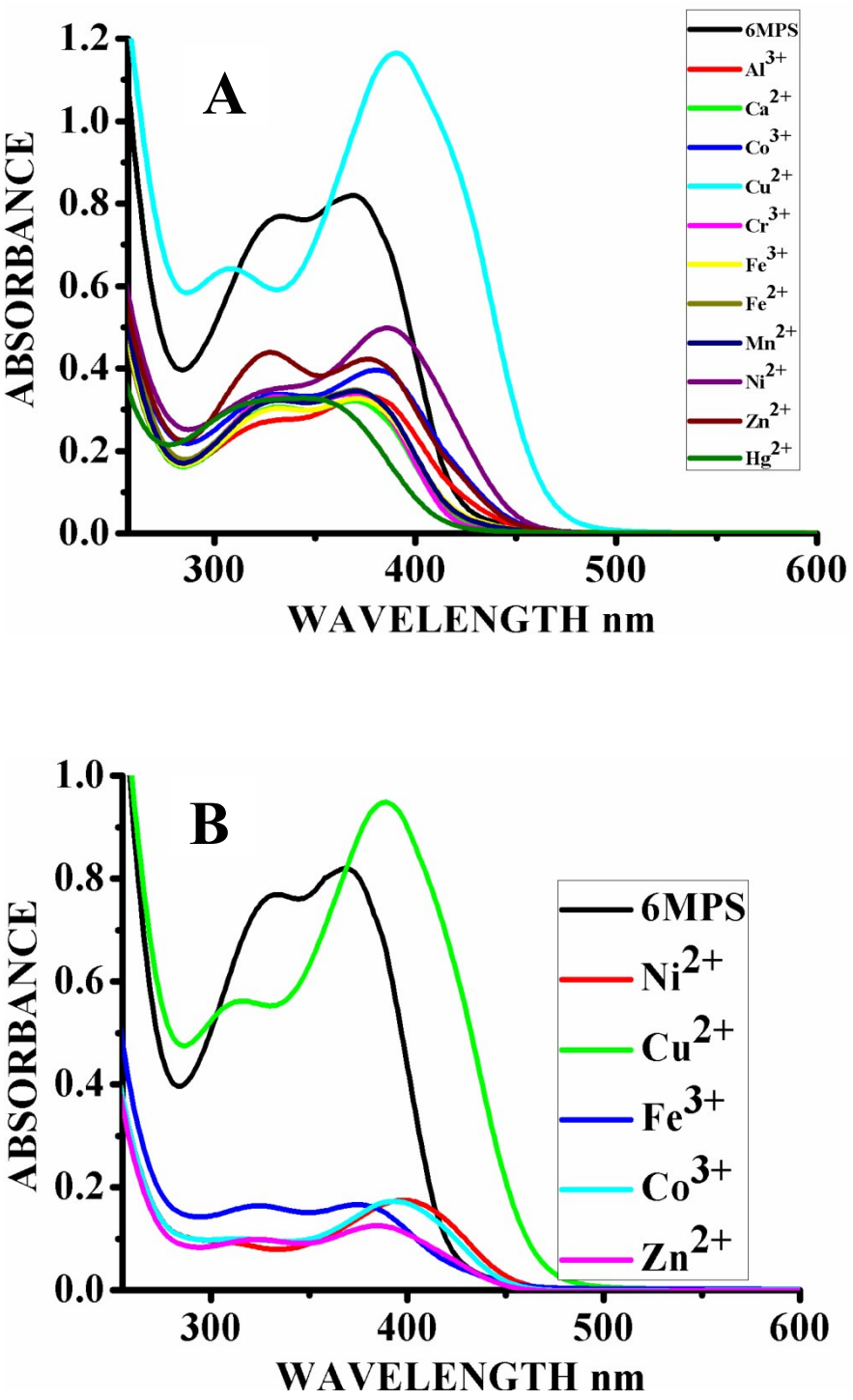

Figure S5 UV-vis absorption spectra of **6MPS** (10 μM, ethanol: H_2O (1: 5)) in the presence of aqueous solution of various chloride and nitrate salts of cations in 10 μM concentration. **A**) Al^{3+}, Ca^{2+}, Co^{3+}, Cr^{3+}, Fe^{3+}, Fe^{2+}, Mn^{2+}, Ni^{2+},Zn^{2+}, Hg^{2+}, $Cu^{2+}$and Co^{2+}.**B**) Co^{3+}, Fe^{3+},Cu^{2+}, Ni^{2+} and Zn^{2+}.

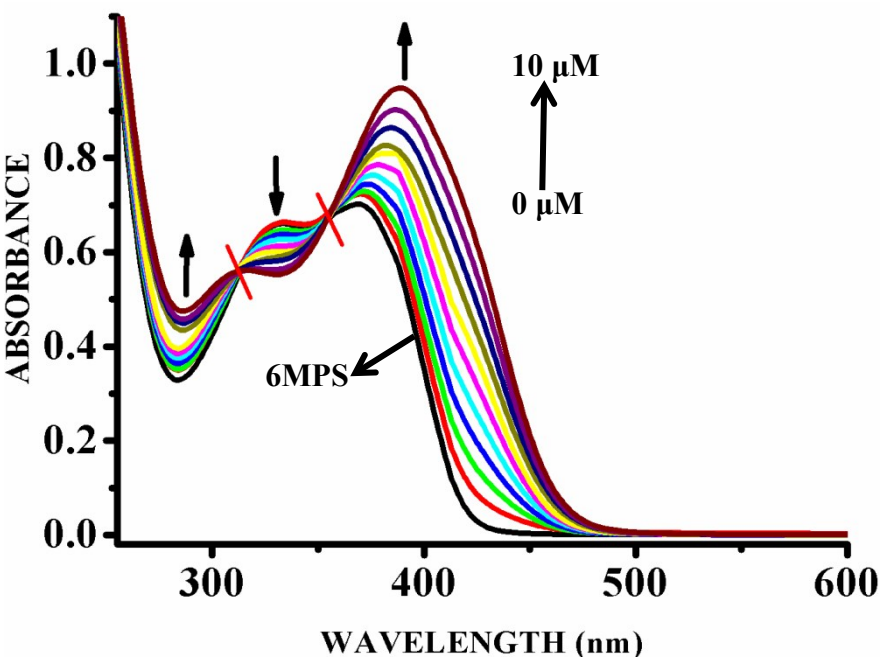

Figure S6 Changes in the absorption spectrum of **6MPS** (10 µM, ethanol: water (1: 5)) upon gradual addition of aqueous solution of copper nitrate in 10 µM concentration.

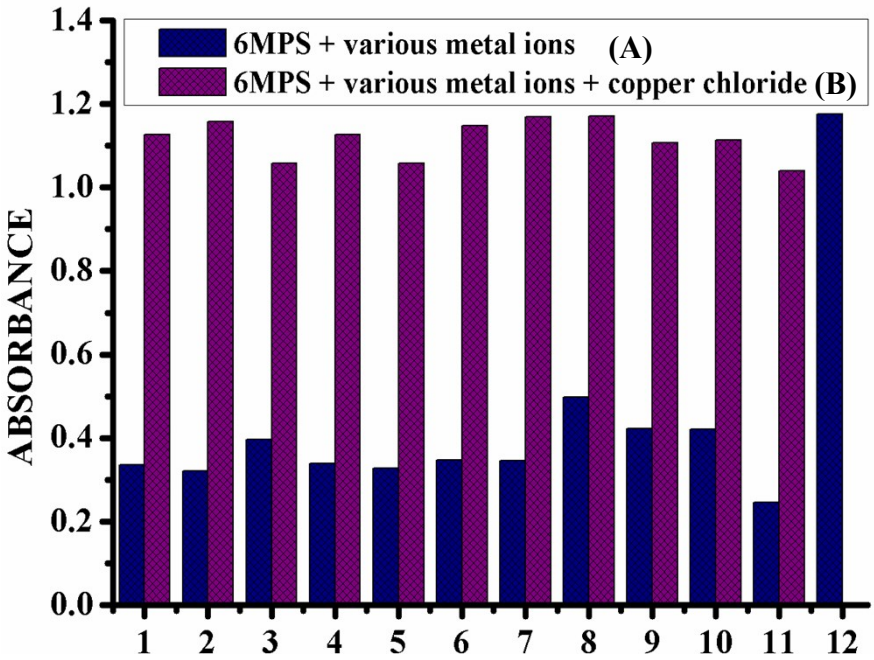

Figure S7 Changes in the absorption spectral intensity of **6MPS** (10 μM, ethanol: H_2O (1: 5)) in the presence of **A**) upon addition of various chloride salts of cations in 10 μM concentration; 1- Al^{3+}, 2- Ca^{2+}, 3- Co^{3+}, 4- Cr^{3+}, 5- Fe^{3+}, 6- Fe^{2+}, 7- Mn^{2+}, 8- Ni^{2+}, 9- Zn^{2+}, 10- Hg^{2+}, 11- $Co^{2+}$and 12- Cu^{2+}; **B**) upon addition of various chloride salts of cations in 10 μM concentration and aqueous solution of copper chloride in 10 μM concentration; 1- Al^{3+} + Cu^{2+}, 2- Ca^{2+} + Cu^{2+}, 3- Co^{3+} + Cu^{2+}, 4- Cr^{3+} + Cu^{2+}, 5- Fe^{3+} + Cu^{2+}, 6- Fe^{2+} + Cu^{2+}, 7- Mn^{2+} + Cu^{2+}, 8- Ni^{2+} + Cu^{2+}, 9- Zn^{2+} + Cu^{2+}, 10- Hg^{2+} + Cu^{2+} and 12- Co^{2+} + Cu^{2+}.

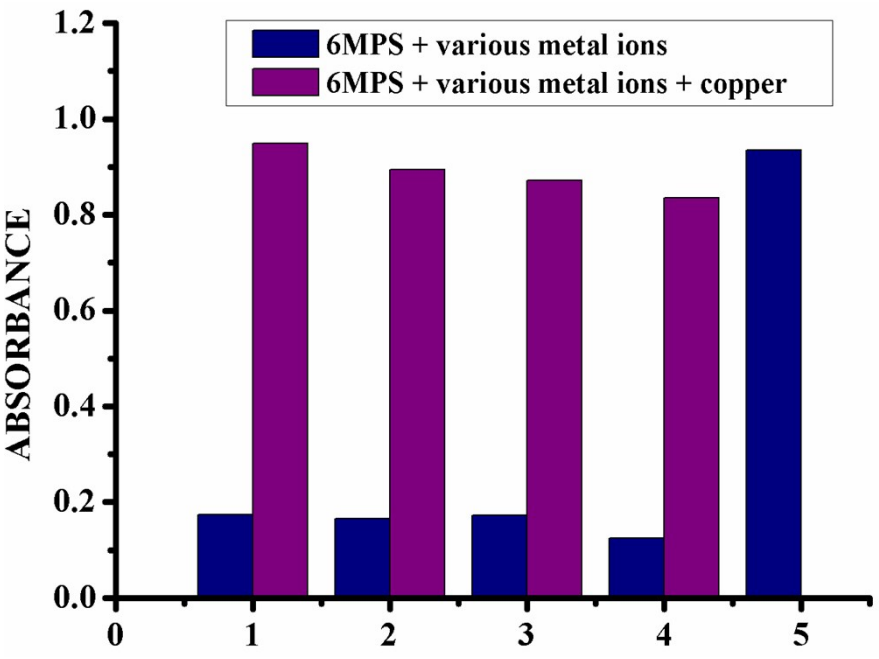

Figure S8 Changes in the absorption spectral intensity of **6MPS** (10 μM, ethanol: H_2O (1: 5)) in the presence of **A**) upon addition of various nitrate salts of cations in 10 μM concentration;1- Co^{3+}, 2- Fe^{3+}, 3- Ni^{2+}, 4- Zn^{2+} and 5- Cu^{2+}. **B**) Aqueous solution of various chloride salts of cations in 10 μM concentration and aqueous solution of copper chloride in 10 μM concentration; 1- Co^{3+}+ Cu^{2+}, 2- Fe^{3+}+ Cu^{2+}, 3- Ni^{2+}+ Cu^{2+}, 4- Zn^{2+}+ Cu^{2+} and 5- Cu^{2+}+ Cu^{2+}.

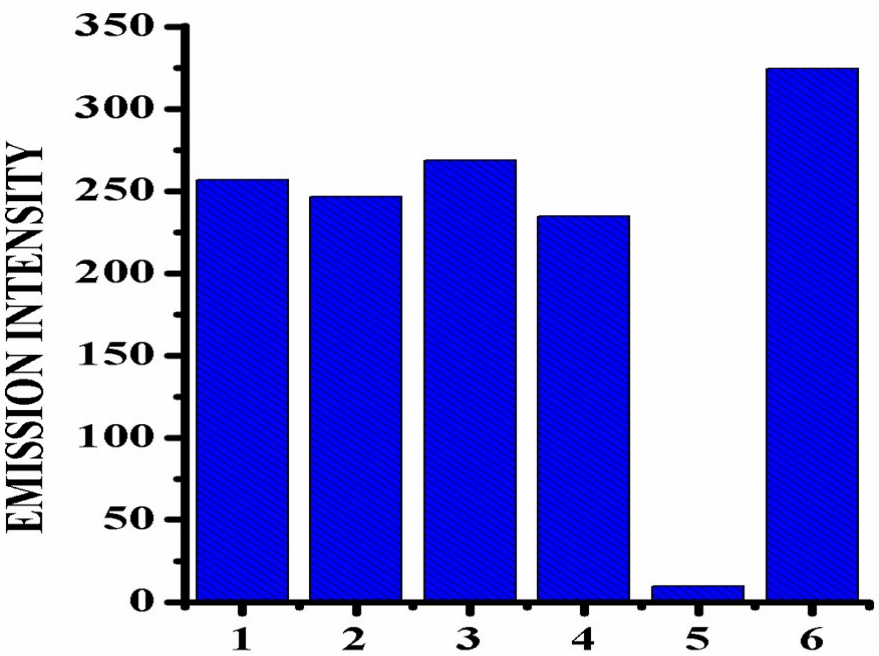

Figure S9 Changes in the fluorescence emission intensity of **6MPS** (10 μM, ethanol: H_2O (1: 5)) upon addition of various nitrate salts of cations (10 μM); 1- Co^{3+}, 2- Fe^{3+}, 3- Ni^{2+}, 4- Zn^{2+}, 5- Cu^{2+} in aqueous solution and 6- blank (**6MPS**).

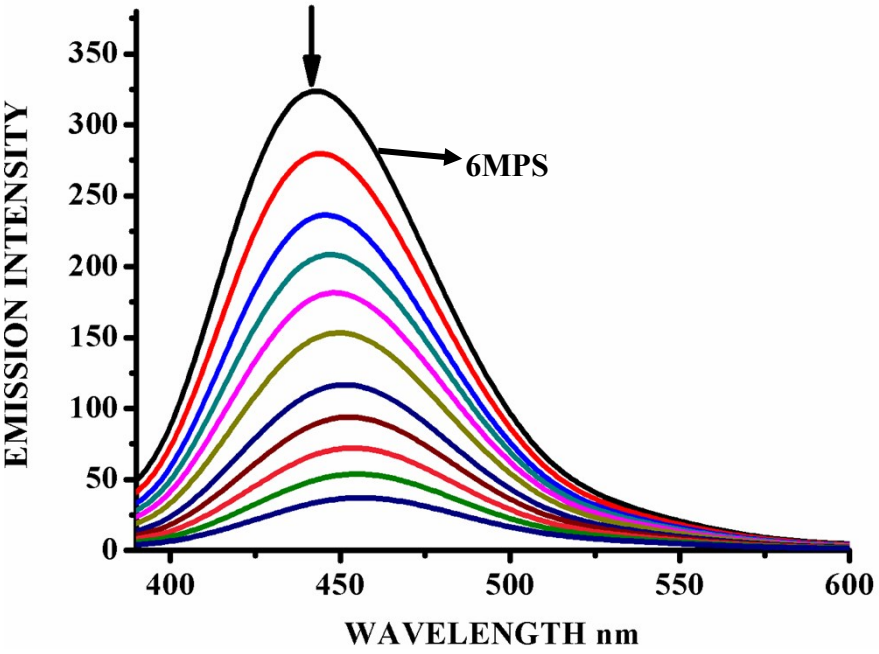

Figure S10 Changes in the fluorescence emission spectrum of **6MPS** (10 μM, ethanol: water (1:5)) upon gradual addition of copper nitrate in 10 μM concentration.

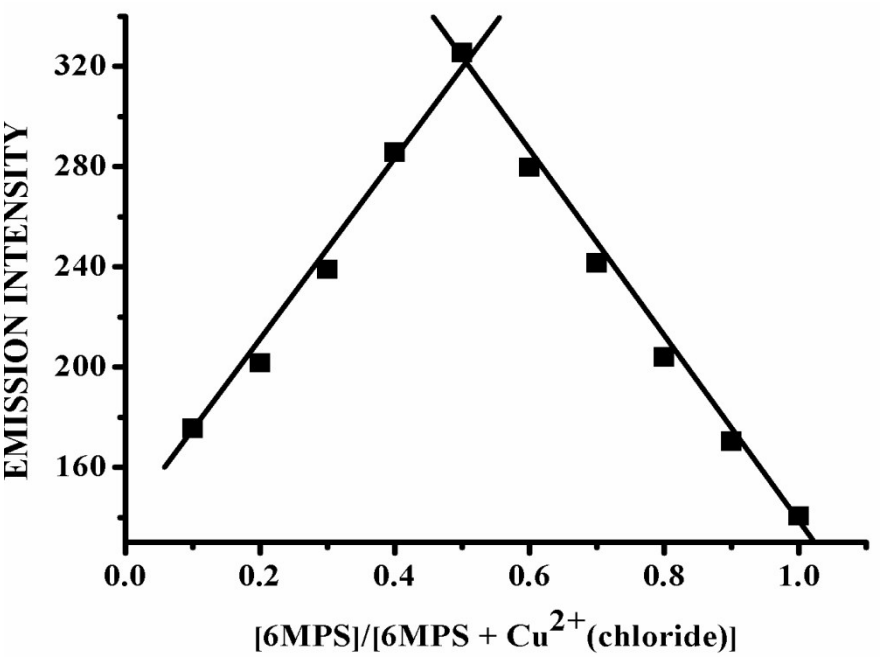

Figure S11 Job's plot of **6MPS** ethanol: water (1:5) and Cu^{2+} ([**6MPS**] + [Cu^{2+} (chloride)] in aqueous solution 10 μM).

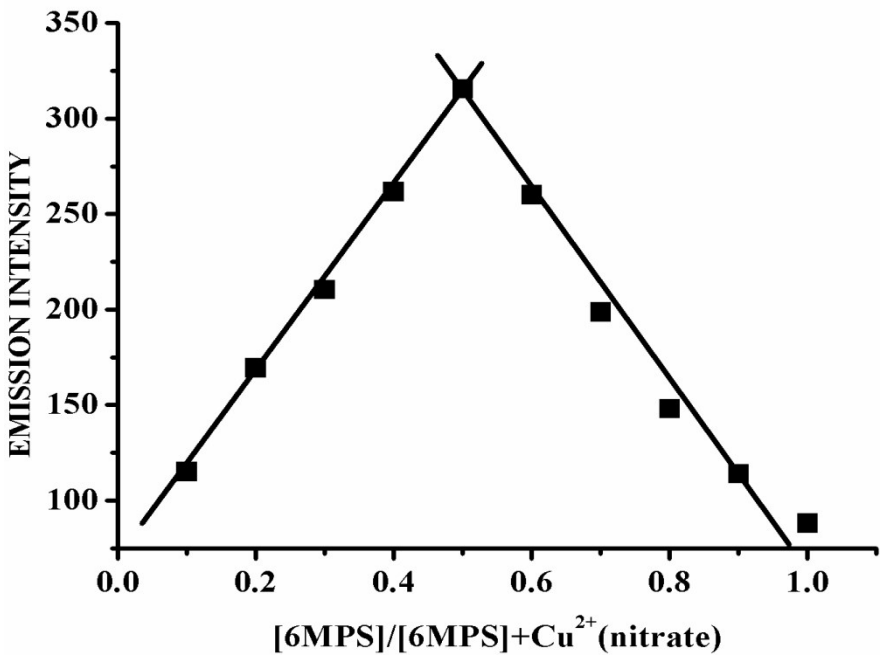

Figure S12 Job's plot of **6MPS** ethanol: water (1:5) and Cu^{2+} ([**6MPS**] + [Cu^{2+} (nitrate)] in aqueous solution 10 μM).

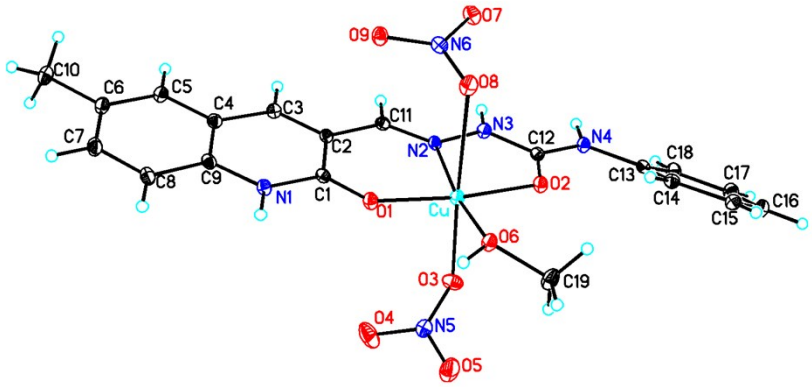

Figure S13. Psuedo octahedral geometry of 6MPSCN

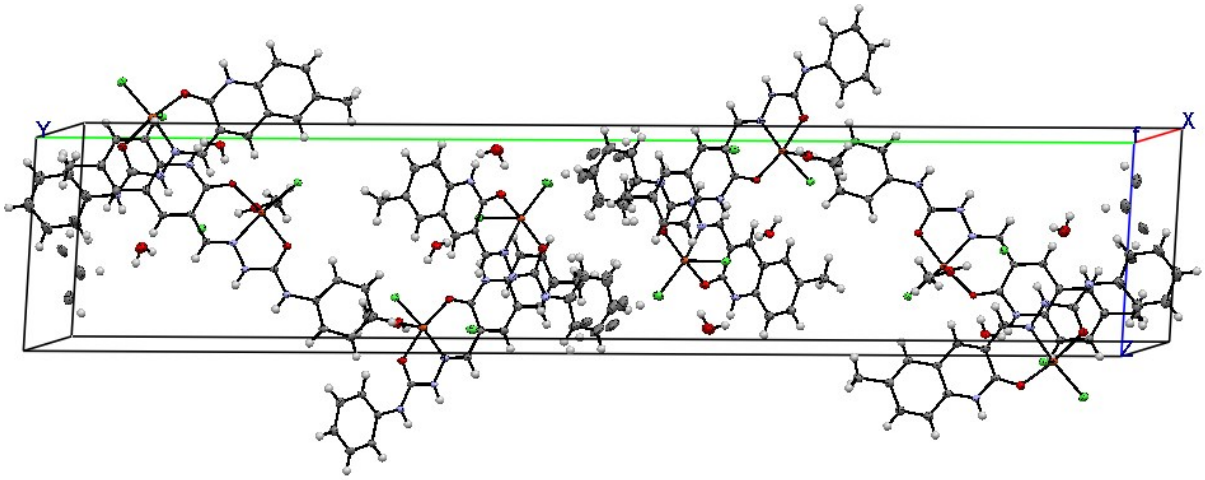

Figure S14 Molecular packing diagram for **6MPSC**.

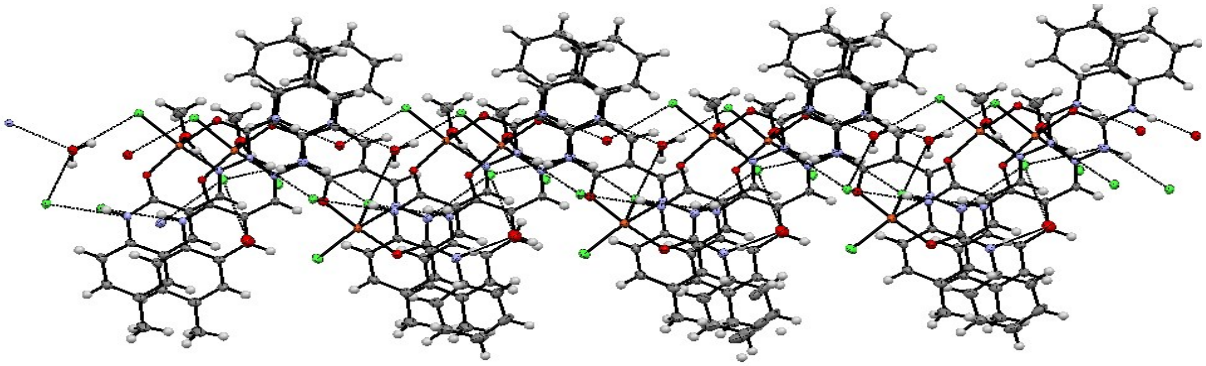

Figure S15 Hydrogen bonding diagram for **6MPSC**.

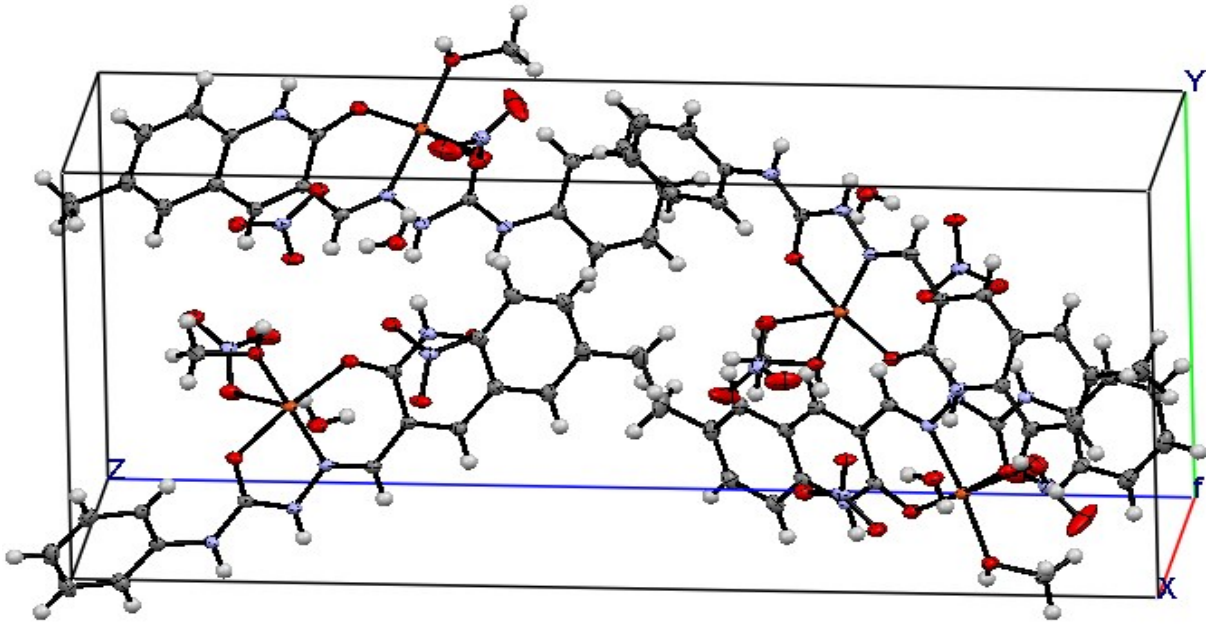

Figure S16 Molecular packing diagram for **6MPSCN**

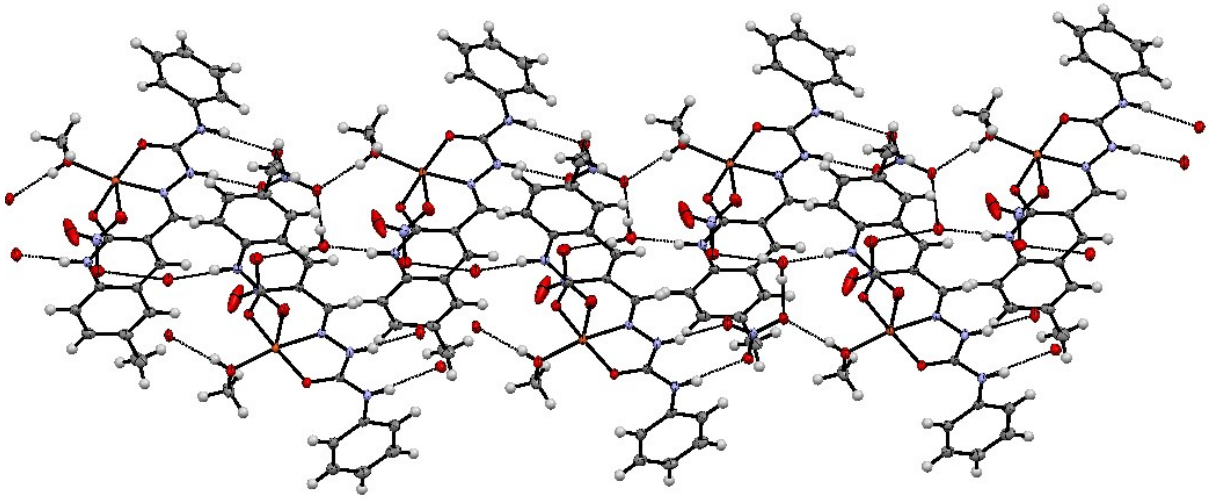

Figure S17 Hydrogen bonding diagram for **6MPSCN.**

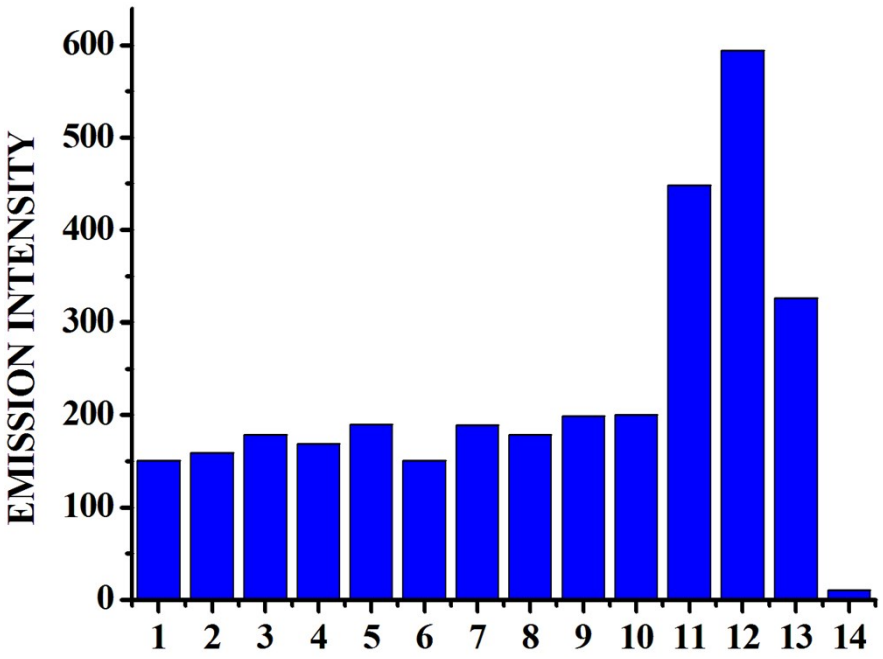

Figure S18 Fluorescence emission spectra of **6MPSCN** in the presence of various L-amino acids (amino acids, 10 μM) in aqueous solution, 1- ala; 2- leu; 3- arg; 4- val; 5- his; 6- aspara; 7- phenyla; 8- thr; 9- pro; 10- glu; 11- asp; 12- met; 13- blank (**6MPS** in ethanol 20 mM, ethanol: water in 1: 5); 14- **6MPSCN**.

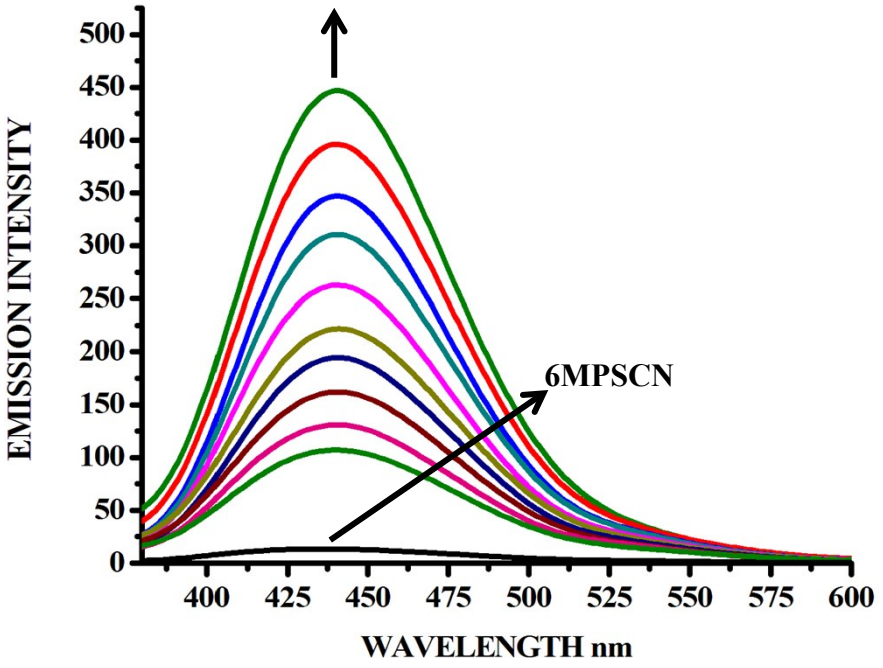

Figure S19 Fluorescence spectra of **6MPSCN** (10 μM) upon gradual addition of aqueous solution of methionine in 10 μM concentration.

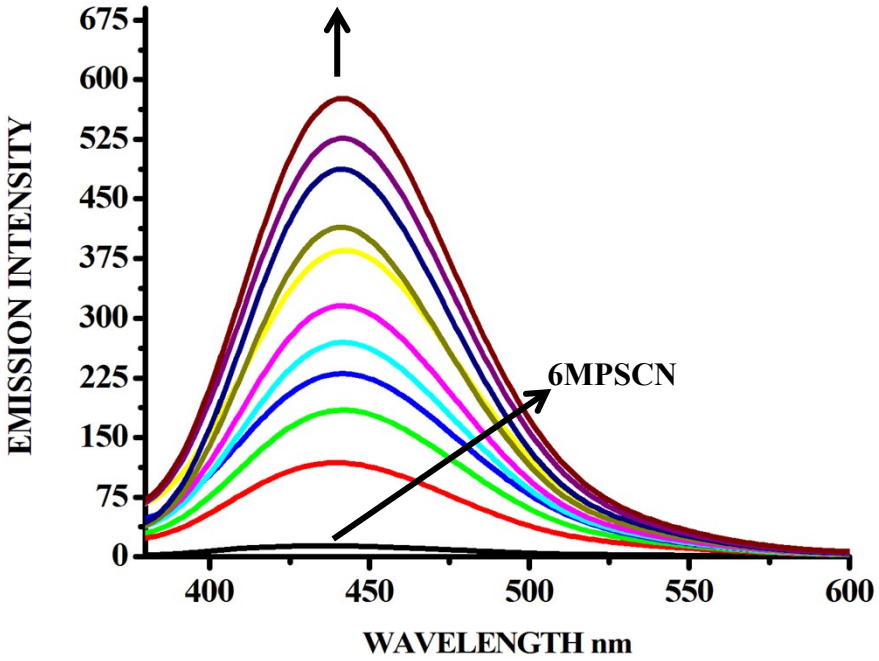

Figure S20 Fluorescence spectra of **6MPSCN** (10 μM) upon gradual addition of aqueous solution of aspartic acid in 10 μM concentration.

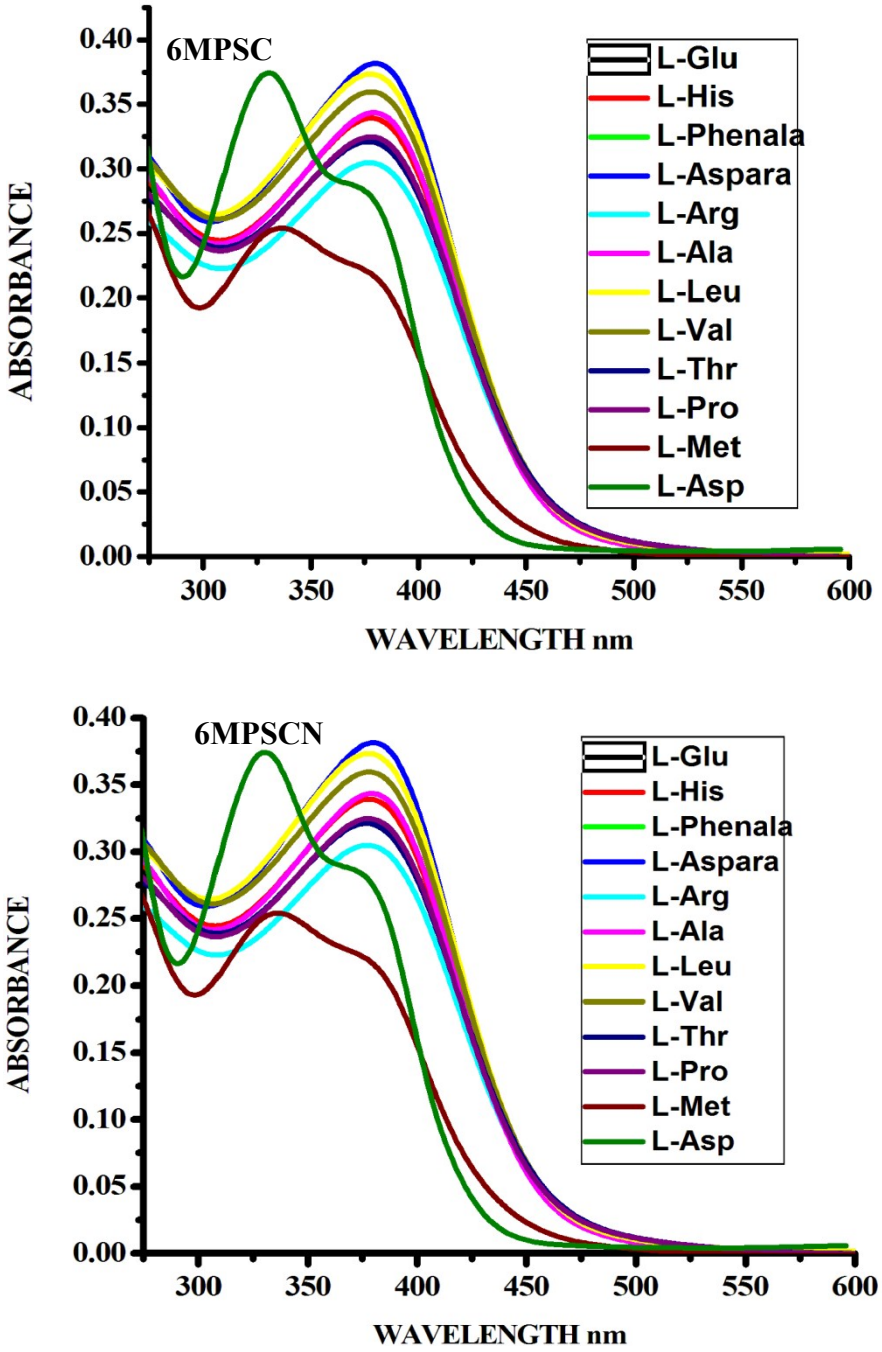

Figure S21 Absorption spectra of **6MPSC** and **6MPSCN** in the presence of various amino acids (all amino acids in 10 μM concentration) in aqueous solution.

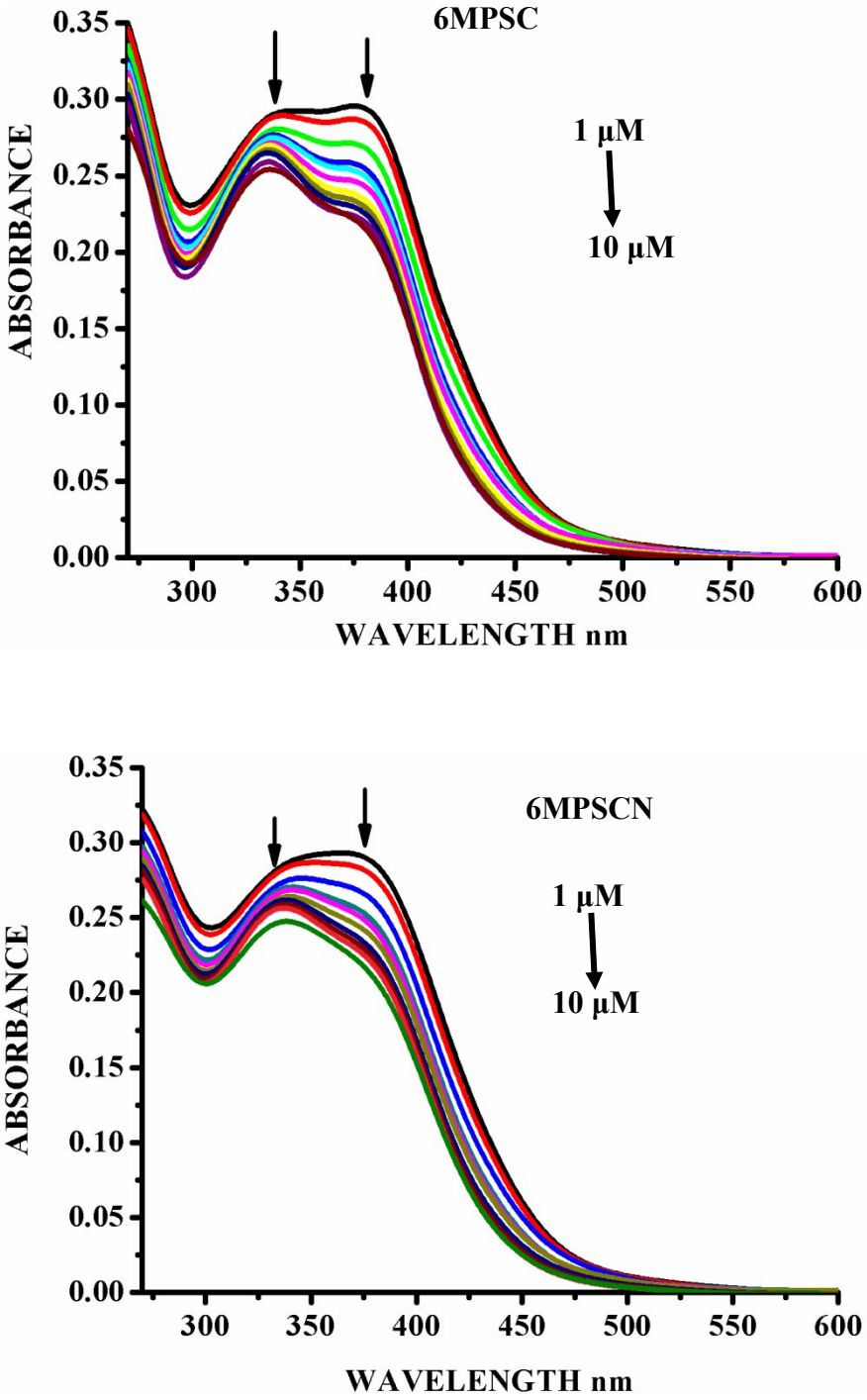

Figure S22 Absorption titration spectra of **6MPSC** and **6MPSCN** (10 µM) upon incremental addition of aqueous solution of methionine in 10 µM concentration.

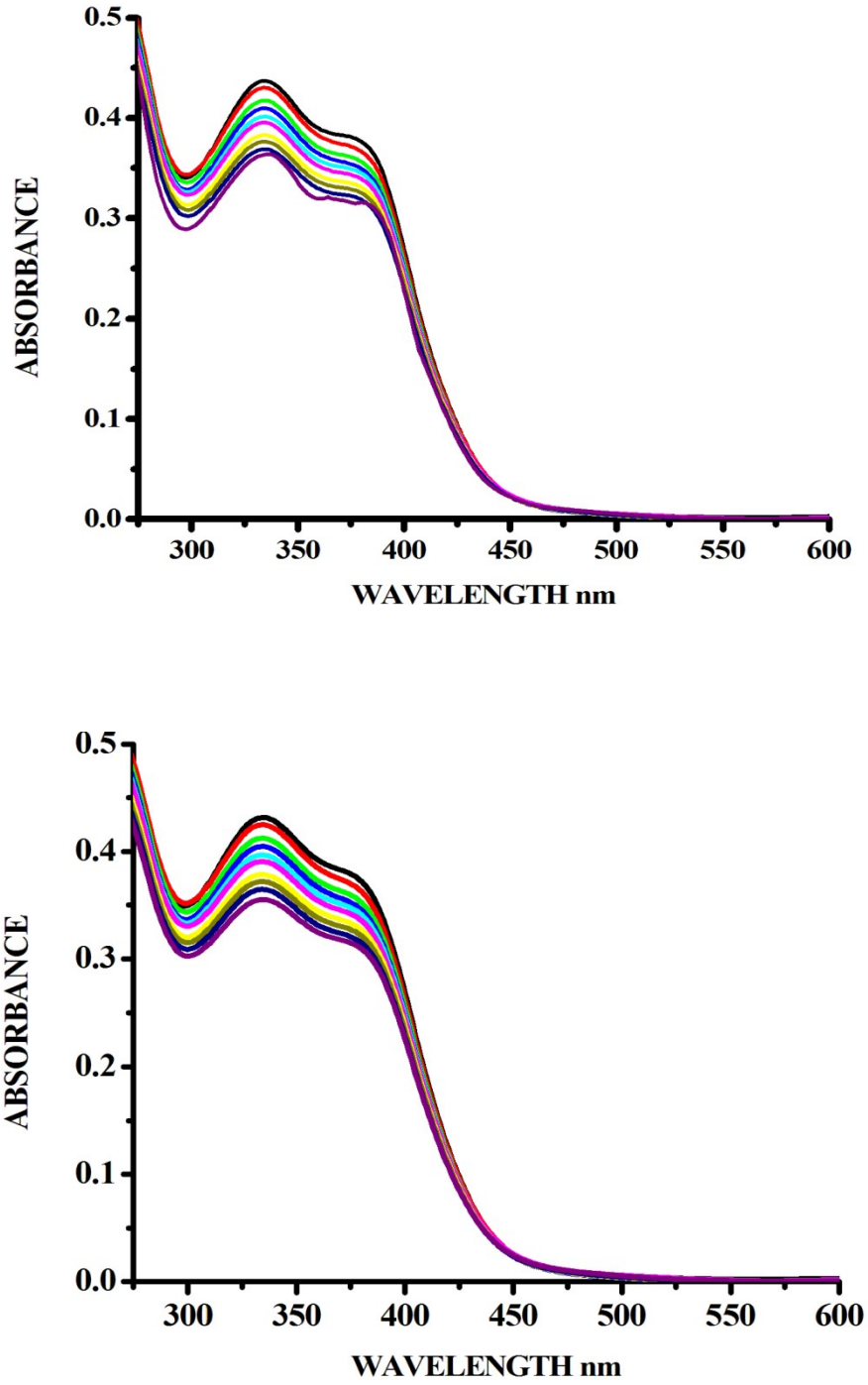

Figure S23 Absorption titration spectra of **6MPSC** and **6MPSCN** (10 μM) upon incremental addition of aqueous solution of aspartic acid in 10 μM concentration.

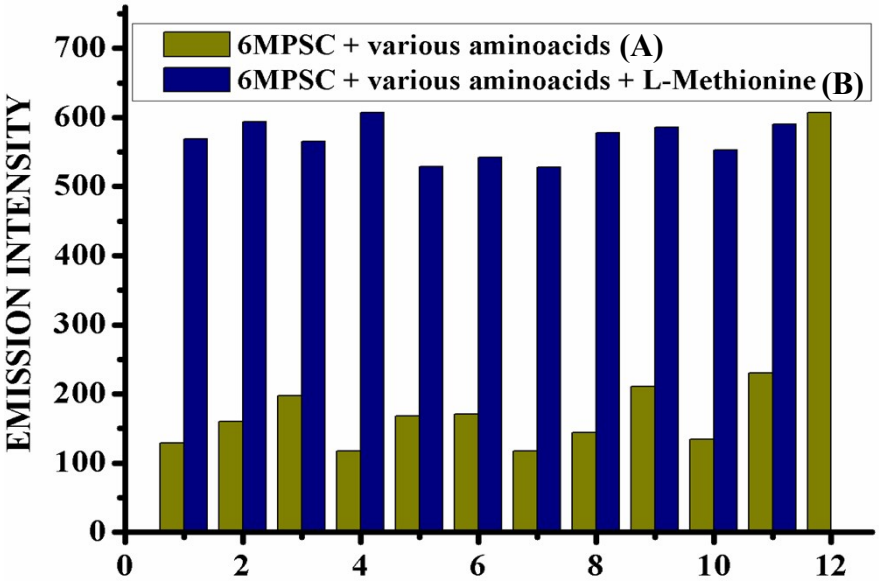

Figure S24 Emission spectra of **6MPSC** (the complex of 10 μM **6MPS** and 10 μM Cu^{2+}) in presence of, **A**)aqueous solution ofvarious amino acids (10 μM), 1- alanine; 2- arginine; 3- valine; 4- asparagine l; 5- leucine; 6- glutamic acid; 7- histidine; 8- phenylanine; 9- proline; 10- threonine and 11- methionine; **B**) aqueous solution of various amino acid (10 μM) and aqueous solution of methionine in 10 μM concentration, 1- 6MPSC + alanine + met; 2- 6MPSC + arginine + met; 3- 6MPSC + valine + met; 4- 6MPSC + asparagine + met; 5- 6MPSC + leucine + met; 6- 6MPSC + glutamic acid + met; 7- 6MPSC + histidine + met; 8- 6MPSC + phenylanine + met; 9- 6MPSC + proline + met; 10- 6MPSC + threonine + met and 11- 6MPSC + met.

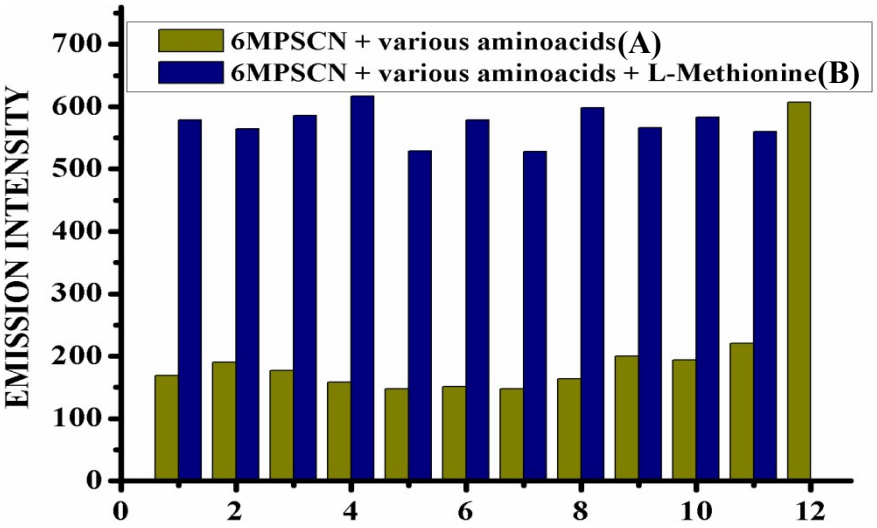

Figure S25 Emission spectra of **6MPSC** (the complex of 10 μM **6MPS**and 10 μM Cu^{2+}) in presence of, **A**) aqueous solution of various amino acids (10 μM), 1- alanine; 2- arginine; 3- valine; 4- asparagine l; 5- leucine; 6- glutamic acid; 7- histidine; 8- phenylanine; 9- proline; 10- threonine and 11- methionine; **B**) aqueous solution of various amino acid (10 μM) and aqueous solution of methionine in 10 μM concentration, 1- 6MPSCN + alanine + met; 2- 6MPSCN + arginine + met; 3- 6MPSCN + valine + met; 4- 6MPSCN + asparagine + met; 5- 6MPSCN + leucine + met; 6- 6MPSCN + glutamic acid + met; 7- 6MPSCN + histidine + met; 8- 6MPSCN + phenylanine + met; 9- 6MPSCN + proline + met; 10- 6MPSCN + threonine + met and 11- 6MPSCN + met.

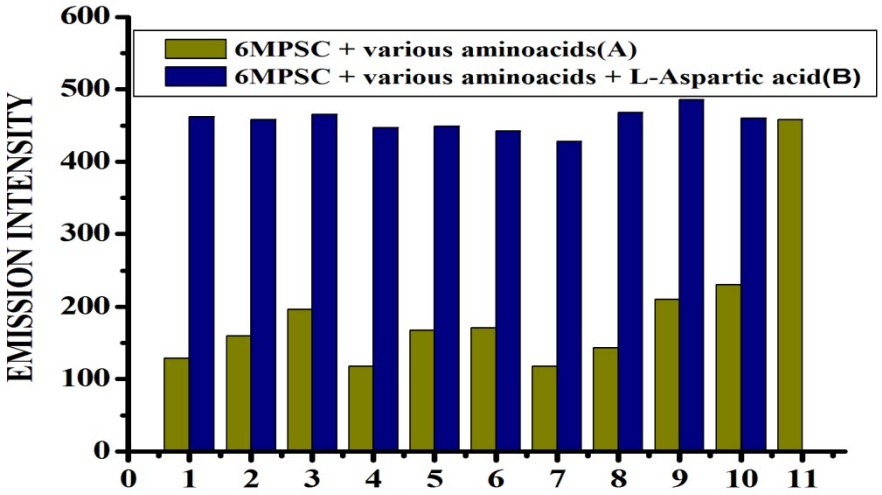

Figure S26 Emission spectra of **6MPSC** (the complex of 10 μM **6MPS** and 10 μM Cu^{2+}) in presence of, **A**) aqueous solution of various amino acids (10 μM), 1- alanine; 2- arginine; 3- valine; 4- asparagine l; 5- leucine; 6- glutamic acid; 7- histidine; 8- phenylanine; 9- proline; 10- threonine and 11- aspartic acid; **B**) aqueous solution of various amino acids (10 μM) and aqueous solution of aspartic acid in 10 μM concentration, 1- 6MPSC + alanine + asp; 2- 6MPSC + arginine + asp; 3- 6MPSC + valine + asp; 4- 6MPSC + asparagine + asp; 5- 6MPSC + leucine + asp; 6- 6MPSC + glutamic acid + asp; 7- 6MPSC + histidine + asp; 8- 6MPSC + phenylanine + asp; 9- 6MPSC + proline + asp; 10- 6MPSC + threonine + asp and 11- 6MPSC + asp.

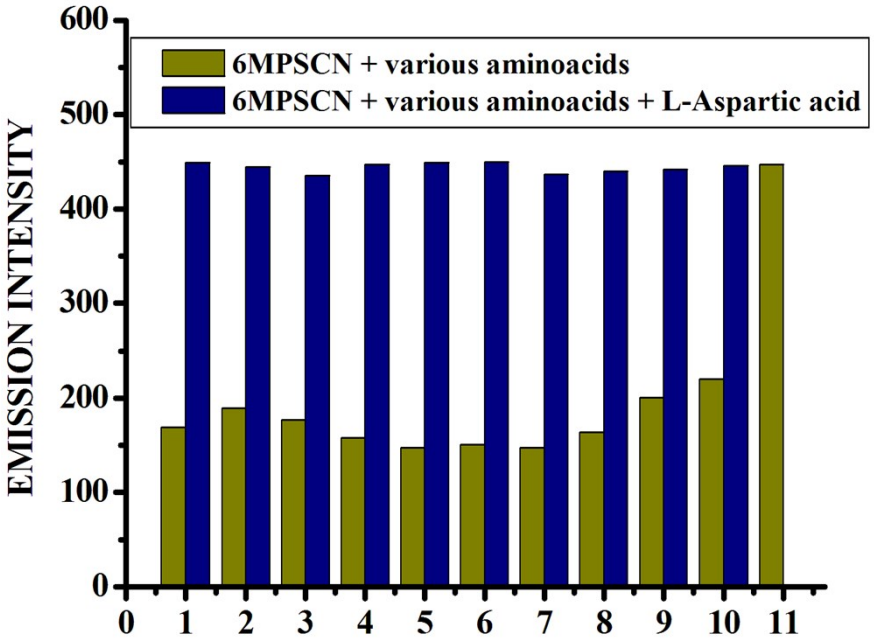

Figure S27 Emission spectra of **6MPSN** (the complex of 10 μM **6MPS** and 10 μM Cu^{2+}) in presence of, **A**) aqueous solution ofvarious amino acids (10 μM), 1- alanine; 2- arginine; 3- valine; 4- asparagine l; 5- leucine; 6- glutamic acid; 7- histidine; 8- phenylanine; 9- proline; 10- threonine and 11- aspartic acid; **B**) aqueous solution of various amino acids (10 μM) and aqueous solution of aspartic acid in 10 μM concentration, 1- 6MPSC + alanine + asp; 2- 6MPSC + arginine + asp; 3- 6MPSC + valine + asp; 4- 6MPSC + asparagine + asp; 5- 6MPSC + leucine + asp; 6- 6MPSC + glutamic acid + asp; 7- 6MPSC + histidine + asp; 8- 6MPSC + phenylanine + asp; 9- 6MPSC + proline + asp; 10- 6MPSC + threonine + asp and 11- 6MPSC + asp.

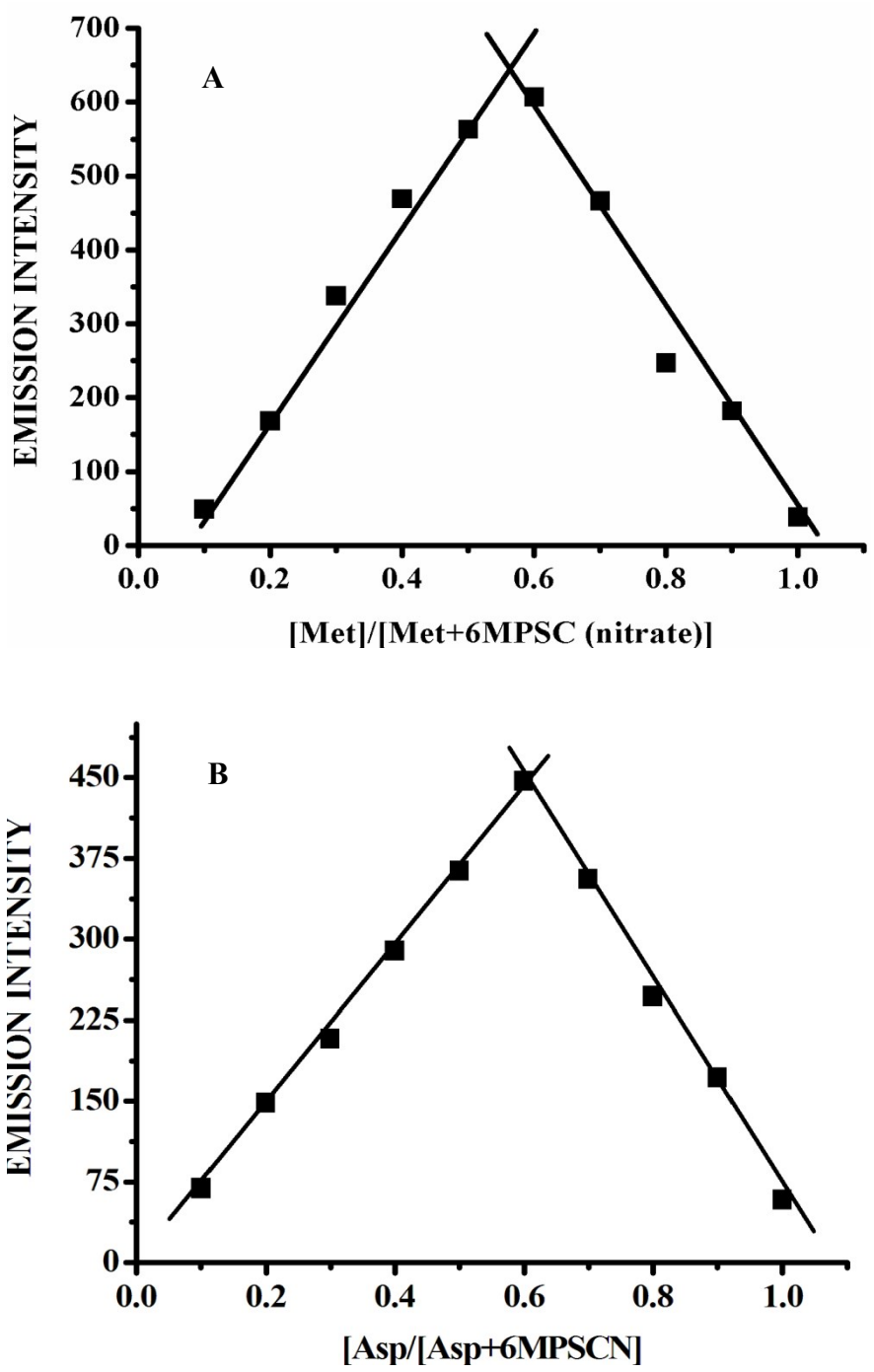

Figure S28 Job's plot of A- **6MPSC** and met ([**6MPSC (nitrate)**] + [met] in aqueous solution 10 μM) B- **6MPSCN** and asp ([**6MPSC (nitrate)**] + [asp]) in aqueous solution 10 μM.

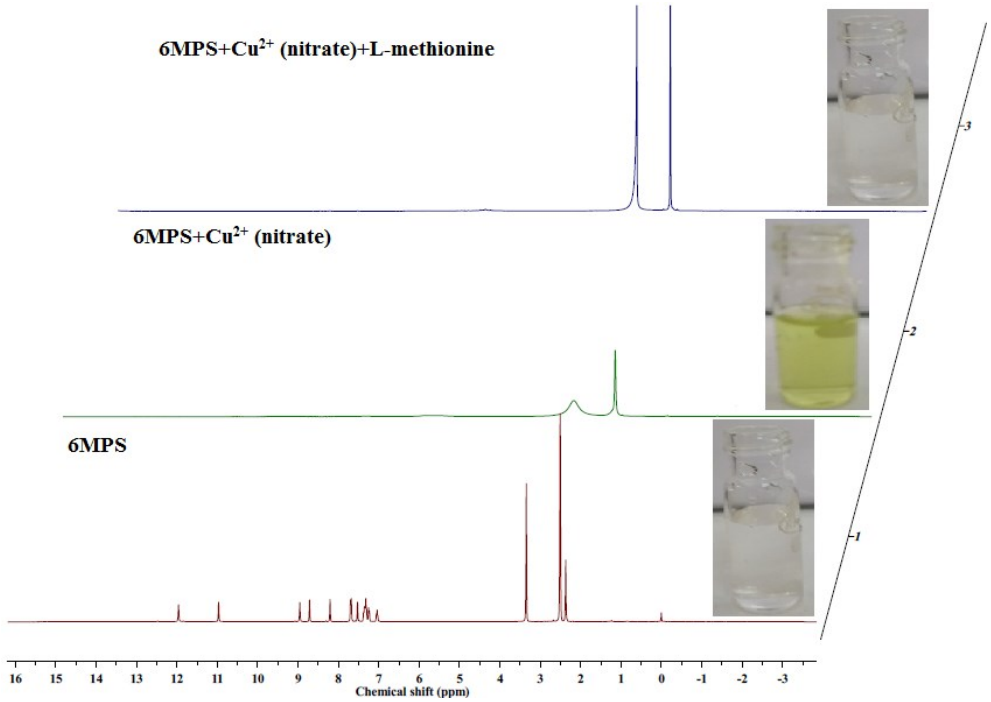

Figure S29 ^{1}H NMR titration (DMSO-d^{6}) spectra for **6MPS** (1.0 eqv), **6MPSCN** (1.0 eqv) and L-methionine (1.0 eqv).

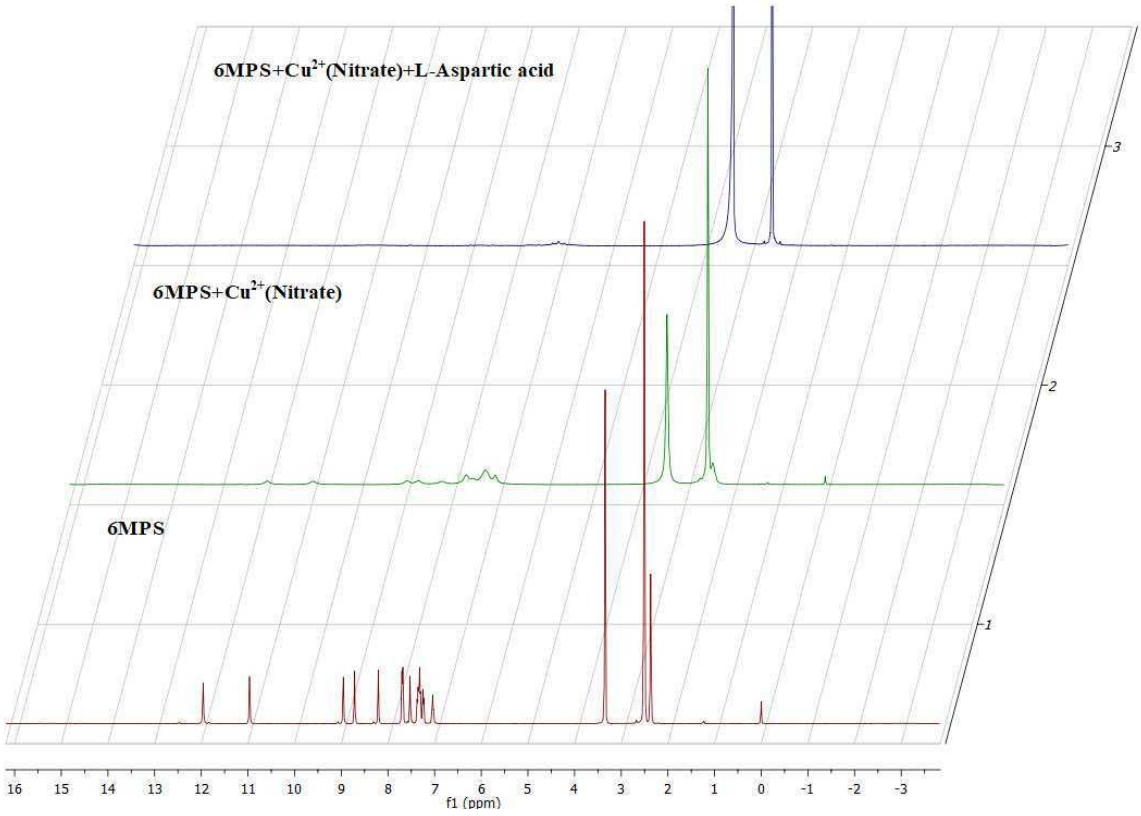

Figure S30 ^{1}H NMR titration (DMSO-d^{6}) spectra for **6MPS** (1.0 eqv), **6MPSCN** (1.0 eqv) and L-aspartic acid (1.0 eqv).

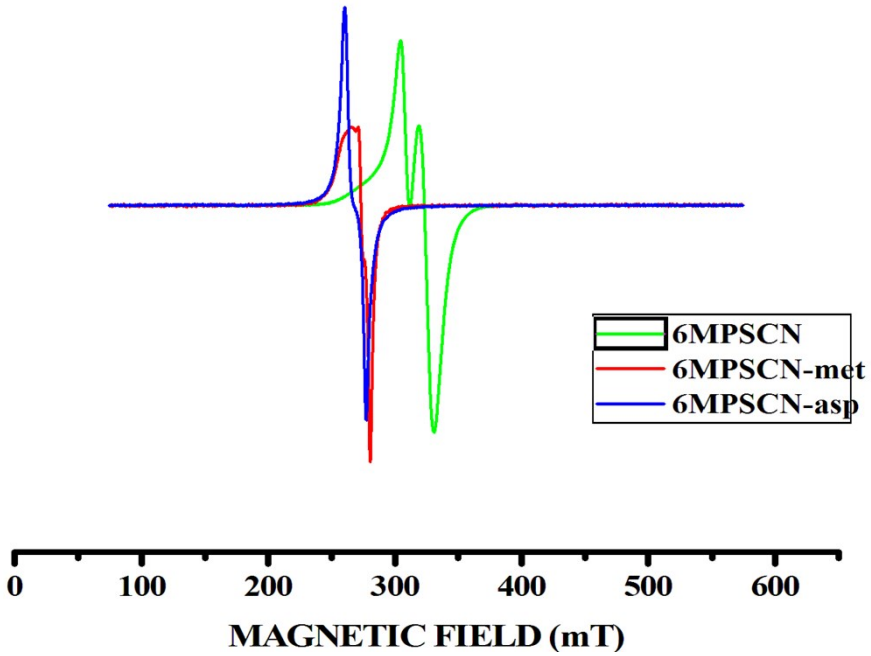

Figure S31 Electron paramagnetic resonance spectra of **6MPSCN**, **6MPSC-met** and **6MPSC-asp**.

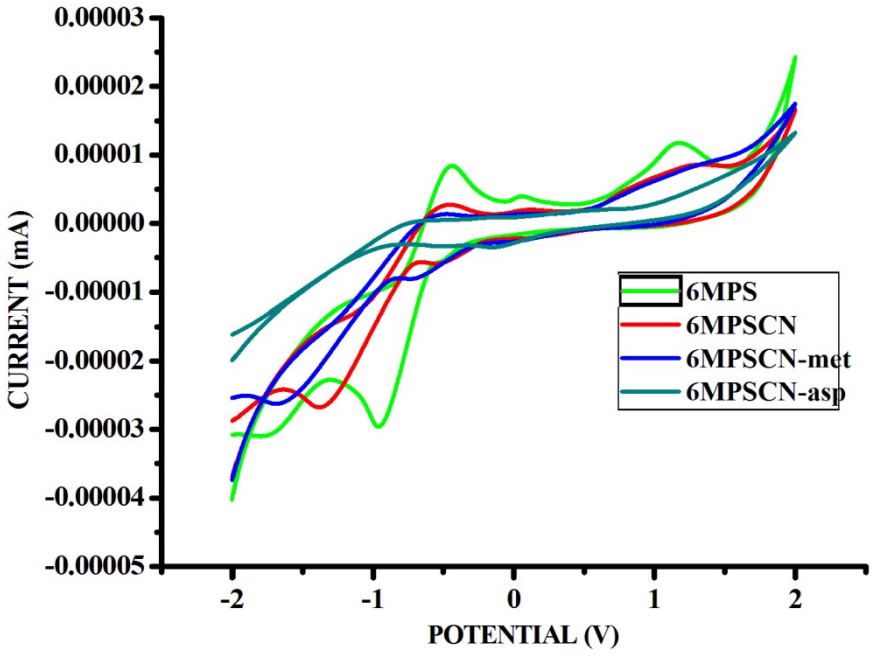

Figure S32 Cyclic voltammograms study in 10 µM concentration of **6MPS**, **6MPSCN, 6MPSCN-met** and **6MPSCN-asp** in DMF solvent using platinum wire counter electrode, platinum disc working electrode and non-aqueous Ag/AgCl reference electrode and tetrabutylammonium perchlorate as supporting electrolyte.

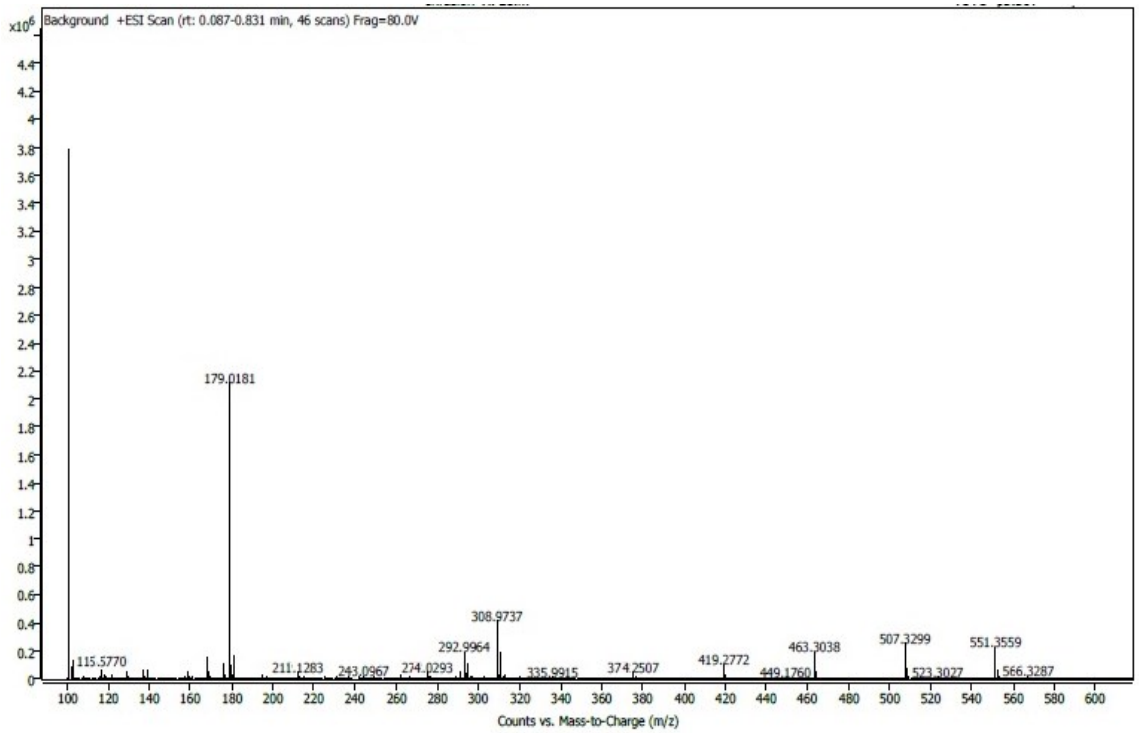

Figure S33 Mass spectra of **6MPSC-met**.

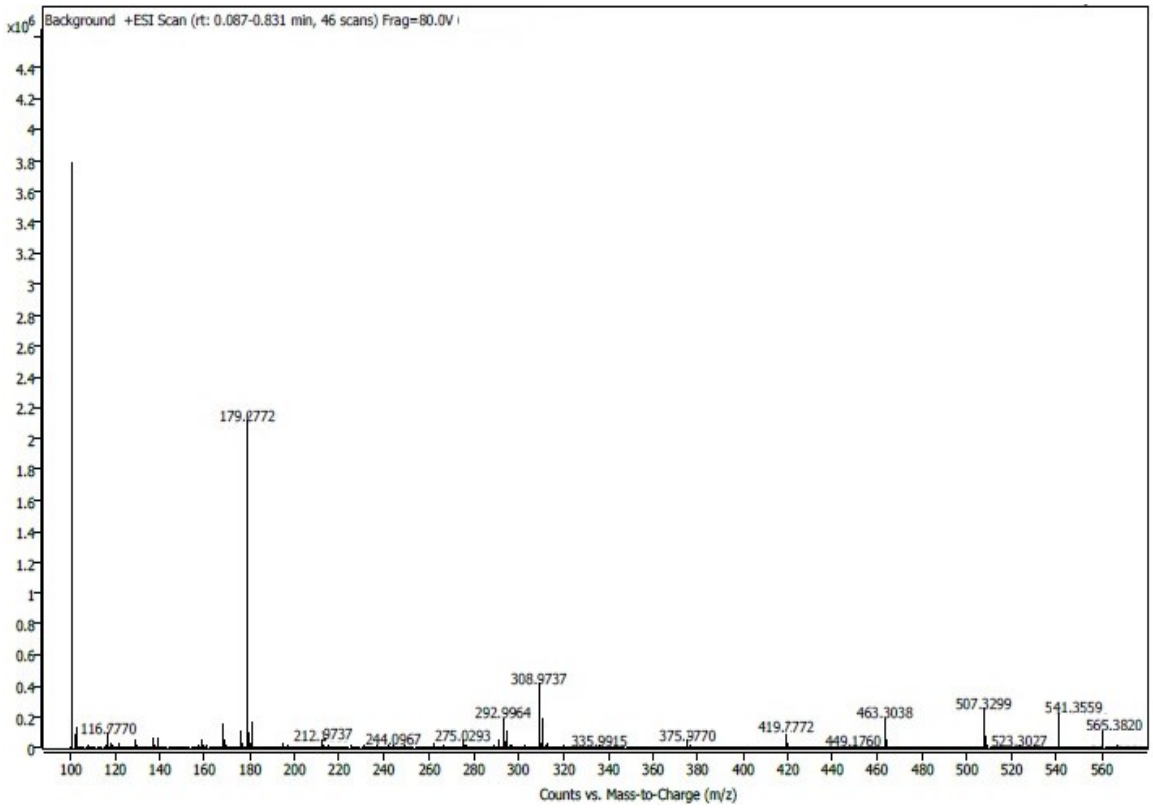

Figure S34 Mass spectra of **6MPSC-asp**.

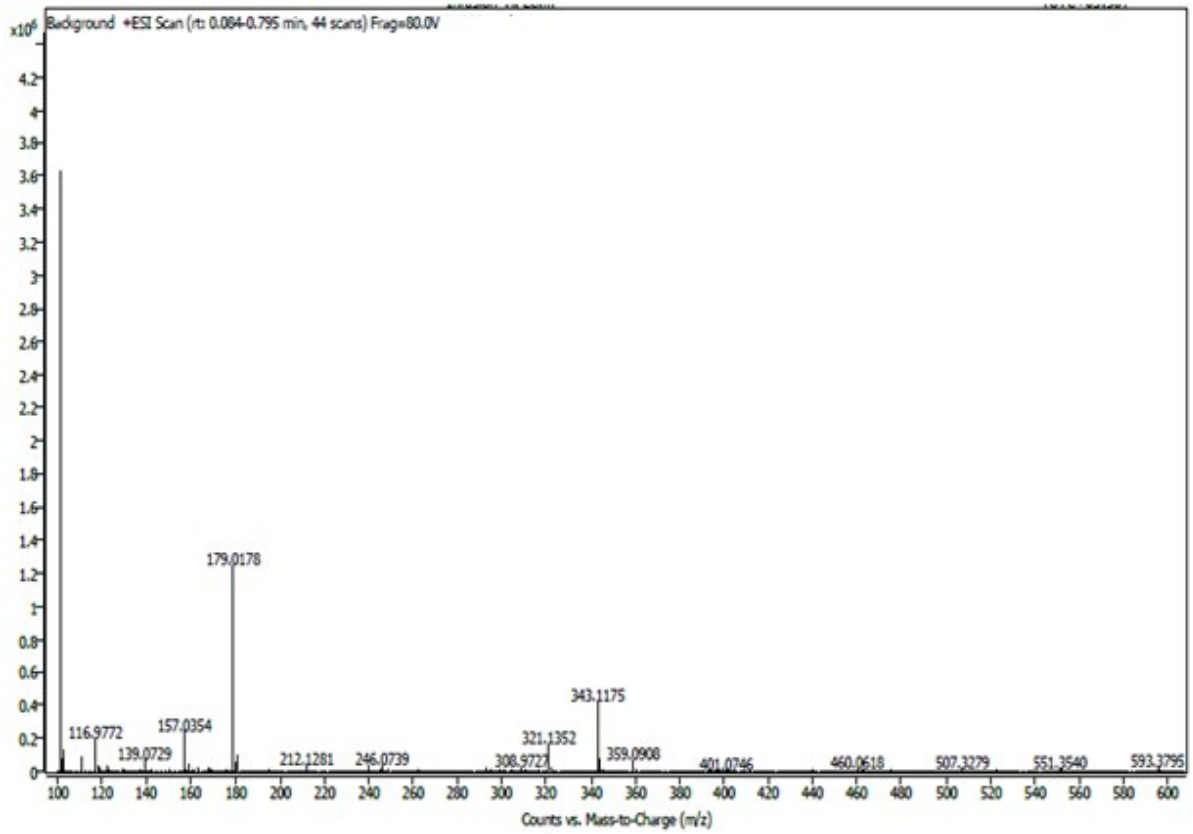

Figure S35 Mass spectra of **6MPSCN-met**.

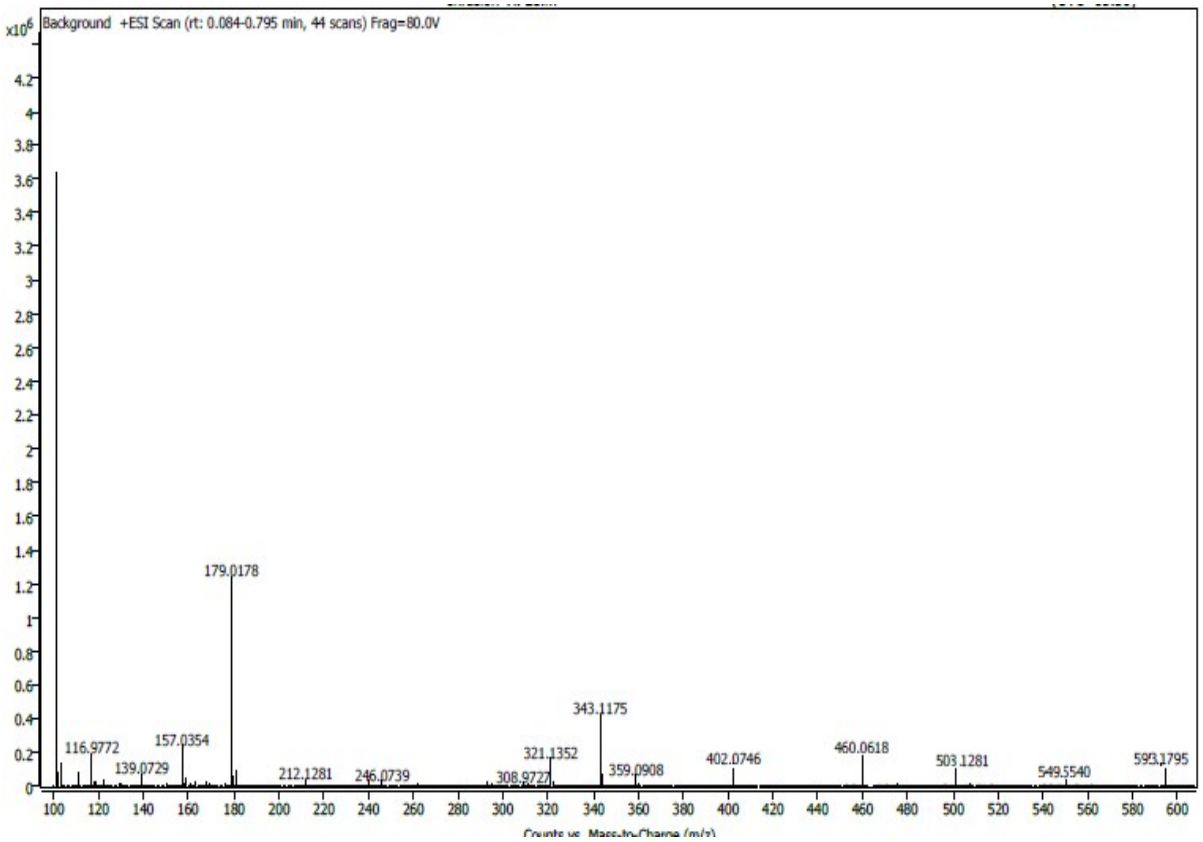

Figure S36 Mass spectra of **6MPSCN-asp**.

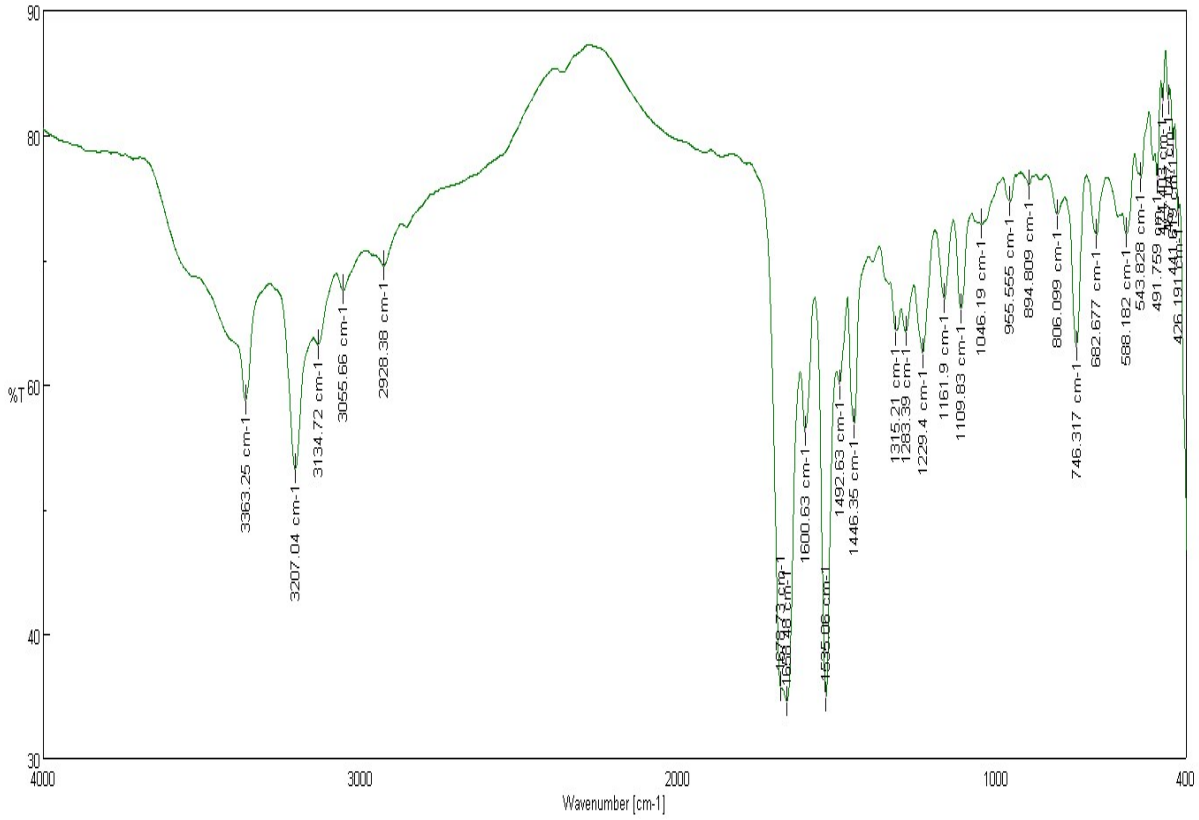

Figure S37 IR spectra of **6MPS**

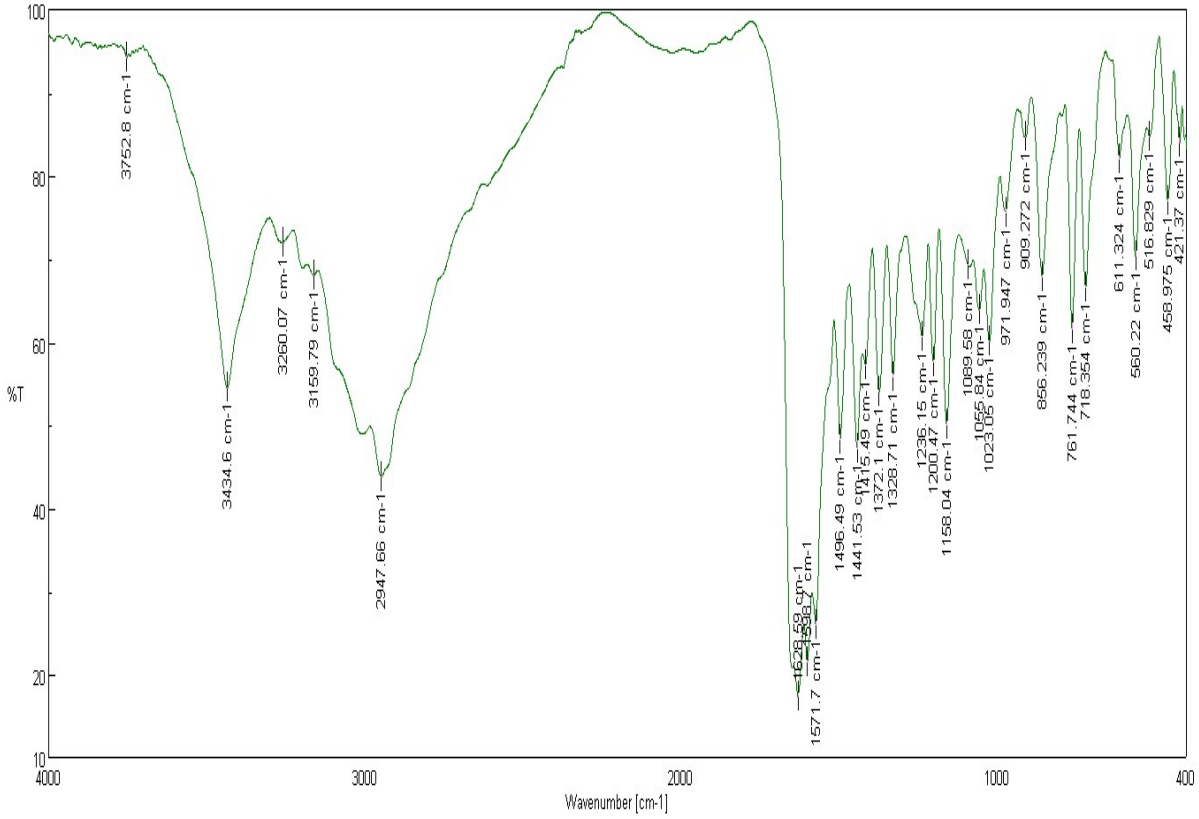

Figure S38 FT IR spectra of **6MPSC**

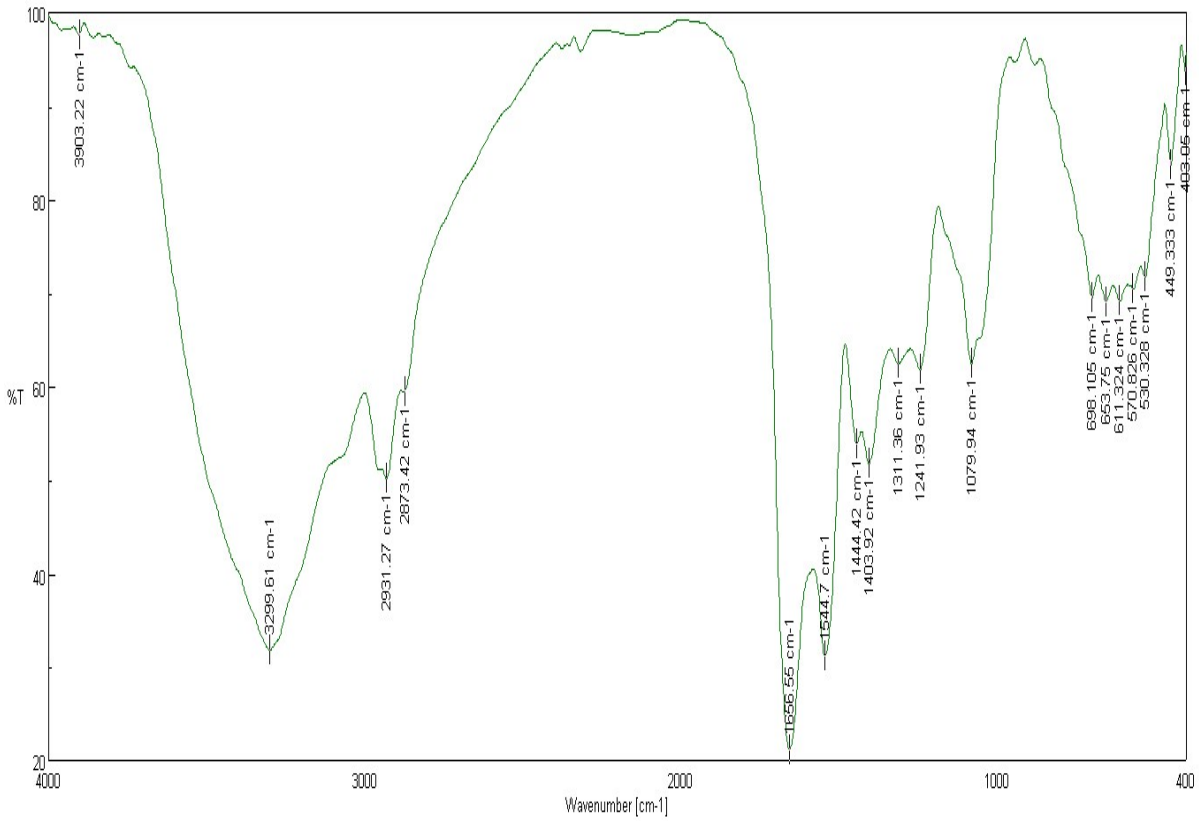

Figure S39 FT IR spectra of **6MPSC-met**

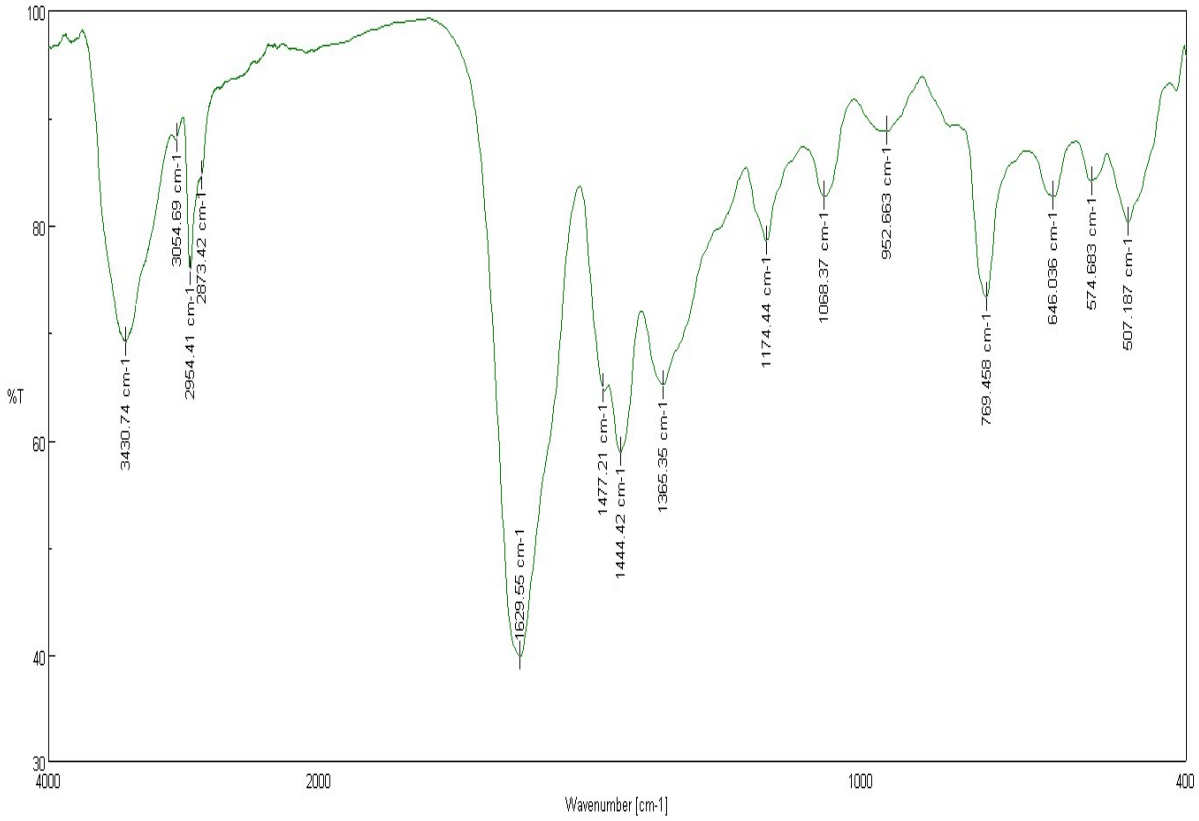

Figure S40 FT IR spectra of **6MPSC-asp**

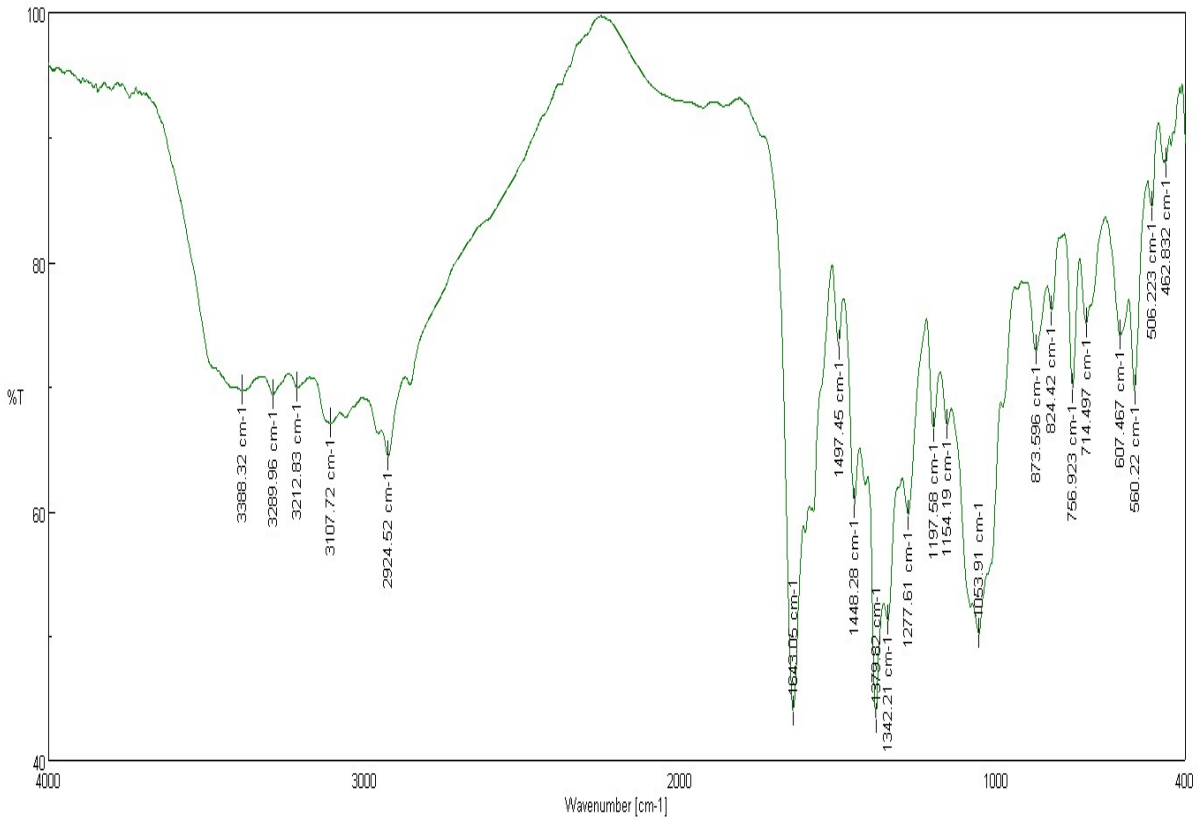

Figure S41 FT IR spectra of **6MPSCN**

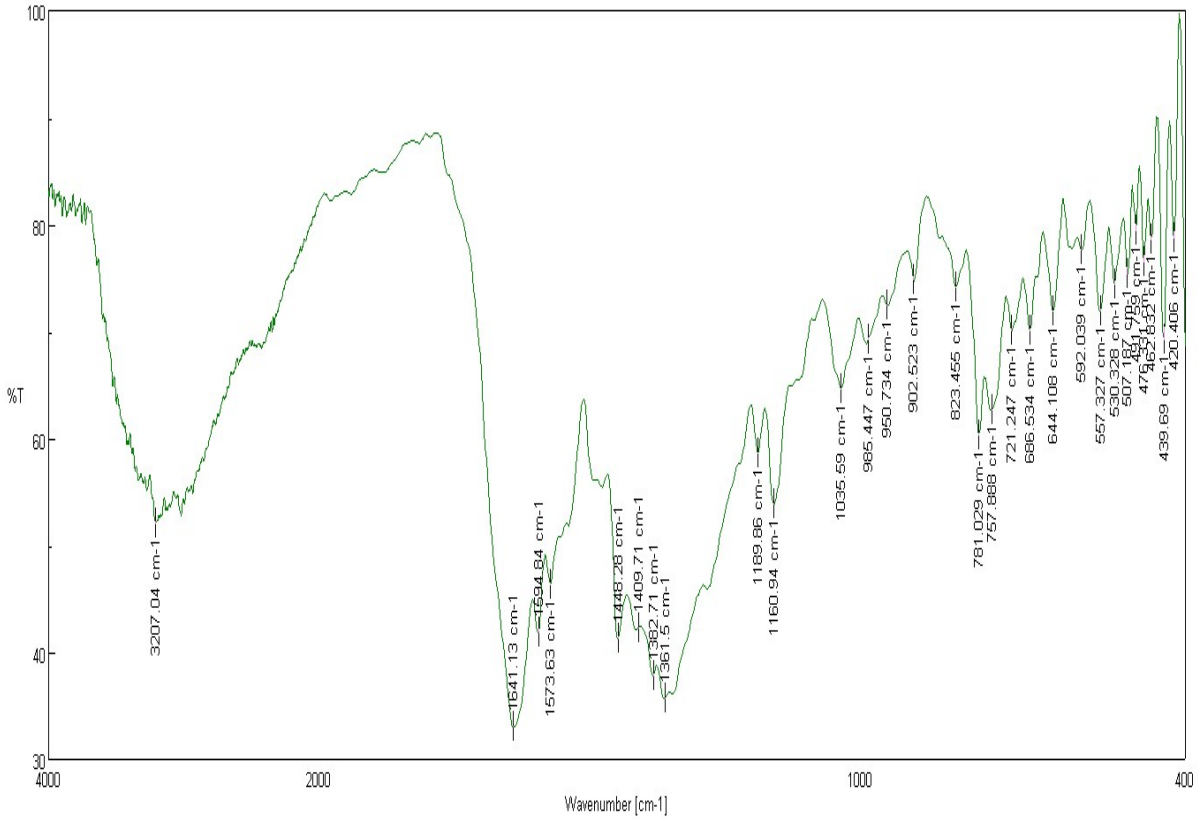

Figure S42 IR spectra of **6MPSCN-met**

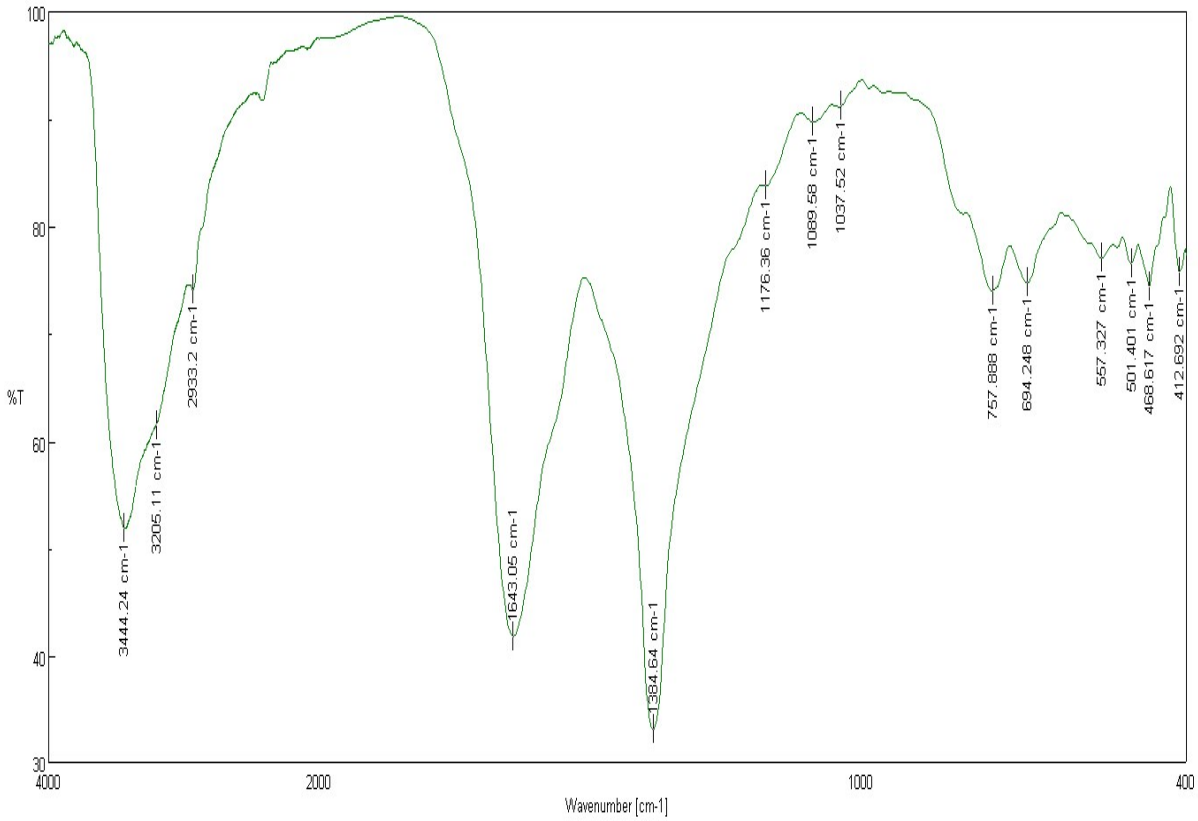

Figure S43 IR spectra of **6MPSCN-asp**

Table S1 Crystallographic data for **6MPS**, **6MPSC** and **6MPSCN**

Compounds	**6MPS**	**6MPSC**	**6MPSCN**
CCDC number	1922255	1922256	1922257
Empirical formula	$C_{18}H_{16}N_4O_2$	$C_{37}H_{40}C_{l4}Cu_2N_8O_7$	$C_{19}H_{22}Cu\ N_6O_{10}$
Formula weight	320.35	977.65	557.96
Temperature	100(2) K	100(2) K	100(2) K
Wavelength	0.71073 Å	1.54178 Å	0.71073 Å
Crystal system	Hexagonal	Monoclinic	Orthorhombic
Space group	P 61	P 21/n	P 21 21 21
a	20.266(2) Å	7.3350(3) Å	7.7584(3) Å
b	20.266(2) Å	54.757(2) Å	11.3260(4) Å
c	20.0904(18) Å	10.2586(4) Å	25.7631(10) Å
α	90°	90°	90°
β	90°	105.497(4)°	90°
γ	120°	90°	90°
Volume	7145.9(15) $Å^3$	3970.5(3) $Å^3$	2263.85(15) $Å^3$
Z	18	4	4
Density (calculated)	1.340 Mg/m^3	1.636 Mg/m^3	1.637 Mg/m^3
Absorption coefficient	0.091 mm^{-1}	4.308 mm^{-1}	1.034 mm^{-1}
F(000)	3024	2000	1148
Theta range for data collection	3.482 to 25.242°	4.545 to 76.838°.	3.539 to 41.150°.
Index ranges	-24<=h<=19, -21<=k<=20, -24<=l<=23	-9<=h<=9, -44<=k<=68, -11<=l<=12	-14<=h<=14, -8<=k<=20, -46<=l<=27
Reflections collected	17444	15292	20976
Independent reflections	8026 [R(int) = 0.1222]	8041 [R(int) = 0.0439]	13561 [R(int) = 0.0386]
Completeness to theta = 25.242	99.4 %	99.4 %	99.6 %
Absorption correction	Semi-empirical from equivalents	Semi-empirical from equivalents	Gaussian
Max. and min. transmission	1.00000 and 0.62928	1.00000 and 0.79706	0.944 and 0.811
Refinement method	Full-matrix least-squares on F^2	Full-matrix least-squares on F^2	Full-matrix least-squares on F^2
Data / restraints / parameters	8026 / 1 / 652	8041 / 42 / 545	13561 / 3 / 339
Goodness-of-fit on F^2	1.016	1.167	1.068
Final R indices [I>2sigma(I)]	R1 = 0.1351, wR2 = 0.3388	R1 = 0.0776, wR2 = 0.1537	R1 = 0.0517, wR2 = 0.0939
R indices (all data)	R1 = 0.2135, wR2 = 0.3987	R1 = 0.0891, wR2 = 0.1580	R1 = 0.0816, wR2 = 0.1120
Extinction coefficient	n/a	n/a	n/a
Largest diff. peak and hole	0.914 and -0.498 $e.Å^{-3}$	0.791 and -0.736 $e.Å^{-3}$	0.742 and -0.997 $e.Å^{-3}$

Table S2 Bond lengths [Å] and bond angles [°] for **6MPSC** and **6MPSCN**

Bond lengths		**Bond angles**	
6MPSC			
Cu(1)-O(1A)	1.974(4)	O(1A)-Cu(1)-N(2A)	90.15(17)
Cu(1)-N(2A)	1.984(4)	O(1A)-Cu(1)-O(2A)	166.37(17)
Cu(1)-O(2A)	1.995(4)	N(2A)-Cu(1)-O(2A)	80.12(17)
Cu(1)-Cl(1)	2.2169(15)	O(1A)-Cu(1)-Cl(1)	93.53(12)
Cu(1)-Cl(2)	2.6990(16)	N(2A)-Cu(1)-Cl(1)	168.66(14)
Cu(2)-O(1B)	1.962(4)	O(2A)-Cu(1)-Cl(1)	94.33(12)
Cu(2)-N(2B)	1.971(4)	O(1A)-Cu(1)-Cl(2)	96.46(12)
Cu(2)-O(2B)	1.986(4)	N(2A)-Cu(1)-Cl(2)	90.20(13)
Cu(2)-Cl(3)	2.2209(14)	O(2A)-Cu(1)-Cl(2)	93.12(12)
Cu(2)-O(3B)	2.407(4)	Cl(1)-Cu(1)-Cl(2)	100.02(6)
		O(1B)-Cu(2)-N(2B)	91.09(16)
		O(1B)-Cu(2)-O(2B)	170.22(16)
		N(2B)-Cu(2)-O(2B)	80.91(16)
		O(1B)-Cu(2)-Cl(3)	95.60(11)
		N(2B)-Cu(2)-Cl(3)	173.31(13)
		O(2B)-Cu(2)-Cl(3)	92.51(11)
		O(1B)-Cu(2)-O(3B)	87.34(16)
		N(2B)-Cu(2)-O(3B)	87.46(16)
		O(2B)-Cu(2)-O(3B)	97.70(16)
		Cl(3)-Cu(2)-O(3B)	93.06(11)
		O(1B)-Cu(2)-Cl(4)	77.90(12)
		N(2B)-Cu(2)-Cl(4)	83.99(13)
		O(2B)-Cu(2)-Cl(4)	95.69(13)
		Cl(3)-Cu(2)-Cl(4)	97.17(5)
		O(3B)-Cu(2)-Cl(4)	162.75(11)
6MPSCN			
Cu-O(1)	1.9195(19)	O(1)-Cu-O(6)	91.15(8)
Cu-O(6)	1.9522(19)	O(1)-Cu-N(2)	92.31(8)
Cu-N(2)	1.953(2)	O(6)-Cu-N(2)	169.55(9)
Cu-O(2)	1.9567(18)	O(1)-Cu-O(2)	173.36(8)

Cu-O(3)	2.302(2)	O(6)-Cu-O(2)	93.74(8)
		N(2)-Cu-O(2)	82.11(8)
		O(1)-Cu-O(3)	97.84(8)
		O(6)-Cu-O(3)	96.05(8)
		N(2)-Cu-O(3)	93.25(8)
		O(2)-Cu-O(3)	86.12(8)

Table S3 Hydrogen bonding for **6MPS**, **6MPSC** and **6MPSCN**.

D-H···A	**d(D-H)**	**d(H···A)**	**d(D···A)**	**<(DHA)**
6MPS				
N(1A)-H(1AA)···O(2C)	0.88	1.87	2.744(13)	175.7
N(3A)-H(3AB)···O(1B)	0.88	1.96	2.830(14)	172.4
6MPSC				
N(3B)-H(3BB)···Cl(2)	0.88	2.35	3.196(4)	161.7
N(4B)-H(4BA)···O(2W)	0.88	1.90	2.775(6)	171.1
O(2W)-H(2W2)···Cl(2)	0.81(2)	2.32(3)	3.082(4)	156(5)
N(1A)-H(1AA)···Cl(4)	0.88	2.33	3.200(4)	171.3
N(3A)-H(3AB)···Cl(4)#1	0.88	2.38	3.230(5)	171.3
N(4A)-H(4A)···O(1W)#1	0.75(8)	2.10(8)	2.828(7)	163(8)
N(1B)-H(1BA)···Cl(2)#4	0.88	2.35	3.205(4)	165.2
O(1W)-H(1W1)···Cl(4)	0.81(2)	2.60(12)	3.142(6)	125(12)
O(2W)-H(2W1)···Cl(3)#1	0.811(19)	2.35(2)	3.142(2)	166(6)
O(3B)-H(3B)···Cl(4)#3	0.98(12)	2.13(12)	3.109(5)	173(10)
Symmetry transformations used to generate equivalent atoms: #1 x,y,z-1 #2 x-1,y,z #3 x+1,y,z #4 x,y,z+1				
6MPSCN				
O(6)-H(6)···O(7)	0.72(4)	1.94(4)	2.656(3)	168(4)
O(1W)-H(1W1)···O(3)#1	0.79(2)	2.59(3)	3.158(3)	129(3)
O(1W)-H(1W1)···O(4)#1	0.79(2)	2.03(2)	2.810(3)	171.(4)
O(1W)-H(1W1)···N(5)#1	0.79(2)	2.65(2)	3.38(3)	155(3)

O(1W)-H(1W2)···O(7)	0.82(2)	1.99(2)	2.812(3)	175(3)
N(1)-H(1A)···O(1W)	0.88	1.82	2.790(3)	171.9
N(3)-H(3B)···O(8)#2	0.88	2.11	2.972(3)	167.0
N(4)-H(4A)···O(9)#2	0.95	2.36	2.887(3)	143.5

Symmetry transformations used to generate equivalent atoms:

#1 -x+2,y-1/2,-z+1/2 #2 x,y+1,z #3 x-1,y,z

Table S4. Electrochemical data of 6MPS, 6MPSC, 6MPSCN, 6MPSC-met¸6MPS-asp¸6MPSCN-met¸6MPSCN-asp

	Oxidation				Ligand oxidation				Reduction				Ligand reduction			
	E_{pa} V	E_{pe} V	Δ_{Ep} mV	$E_{1/2}$ V	E_{pa}	E_{pe}	Δ_{Ep}	$E_{1/2}$	E_{pa}	E_{pe}	Δ_{Ep}	$E_{1/2}$	E_{pa}	E_{pe}	Δ_{Ep}	$E_{1/2}$
6MPS					1.115	1.0232	92	1.069	-0.204	0.122	326	0.041	-0.986	-0.398	588	-0.692
6MPSCl	0.026	-	-	-	1.637	1.032	605	1.335	-0.312	-0.502	166	-0.419	-1.326	-1.56	234	-1.443
6MPSCn	0.406	-	-	-	1.396	1.184	212	1.29	0.158	-0.412	285	0.127	-0.584	-1.402	818	-0.993
6MPSCl-Met	-	-	-	-	0.121	-	-	-	-0.738	-0.503	235	-0.621	-	-	-	-
6MPSCl-Asp	0.992	0.496	496	0.744	-	-	-	-	0-089	-0.112	191	-0.023	-0.502	-1.008	506	-0.755
6MPSCn-Met	0.156	-0.178	334	0.011	1.324	1.006	318	1.165	-0.594	-0.748	154	-0.671	-1.398	-1.620	222	-1.509
6MPSCn-Asp	0.051	-0.156	105	0.103	-	1.006	-	-	-	-	-	-	-	-	-	-

Table S5 Elemental analysis and FT-IR spectroscopy of **6MPS**, **6MPSC**, **6MPSCN**, **6MPSC-met**, **6MPSCN-met**, **6MPSC-asp** and **6MPSCN-asp**

Compounds	Elemental analysis Calculated (Found) %				IR spectral data in cm^{-1}					
	C	H	N	S	$\nu_{C=O}$	$\nu_{C=N}$	$\nu_{C=O}$	$\nu_{C=O}$ (asym)	$\nu_{C=O}$ (sym)	ν_{C-S}
6MPS	68.25 (68.23)	5.43 (5.41)	16.76 (16.73)	-	1658	1600	1678	-	-	-
6MPSC	46.31 (46.29)	3.09 (3.05)	11.68 (11.66)	-	1628	1571	1628	-	-	-
6MPSC-met	48.67 (48.65)	4.73 (4.70)	13.41 (13.38)	3.61 (3.58)	1656	1544	1656	1656	1403	698
6MPSC-asp	48.77 (48.75)	4.45 (4.42)	11.22 (11.18)	-	1629	1629	1629	1629	1444	-
6MPSCN	47.75 (47.71)	4.22 (4.18)	14.65 (14.63)	-	1643	1581	1643	-	-	-
6MPSCN-met	51.92 (51.88)	4.93 (4.89)	13.16 (13.14)	6.03 (6.0)	1641	1573	1641	1641	1448	781
6MPSCN-asp	46.32 (46.28)	4.48 (4.45)	12.62 (12.59)	-	1643	1643	1643	1643	1384	-

References

1. F.E. Mabbs and D.J. Machin, *Magnetism, Transition Metal Complexes,* Chapman and Hall: London, 1973.

2. R.H. Blessing, An empirical correction for absorption anisotropy, *Acta Crystallo. Sect*., 1995, **A51** 33-38.

3. G.M. Sheldrick and G. M., SHELXTL Version 5.1, *An Integrated System for Solving, Refining and Displaying Crystal Structures from Diffraction Data*, Siemens Analytical X-ray Instruments, Madison, WI, 1990.

4. X. Li, F. Huo, Y. Yue, Y. Zhang and C.A. Yin, *Sens. Actuators B,* 2017, **253**, 42–49.

5. H. Un, S. Wu, C. Huang, Z. Xuc and L. Xu, *Chem. Commun.,* 2015, **51**, 3143-3146.

6. S. Brenner *Genetics*,1974, **77**, 71–94.

7. A. Mohankumar, G. Shanmugam, D. Kalaiselvi, C. Levenson, S. Nivitha, G. Thiruppathi and P. Sundararaj, *RSC Adv.,*2018, **8**, 33753-33774.

8. T.J. Fabian and T.E. Johnson, *J. Gerontol.,*1994, **49**, B145–B156.

9. G. Devagi, A. Mohankumar, G. Shanmugam, S. Nivitha, F. Dallemer, P. Kalaivani, P. Sundararaj and R. Prabhakaran, *Sci. Rep.,* 2018, **8**, 7688.

10. C. Elamathi, R.J. Butcher and R. Prabhakaran, *Appl. Organomet. Chem.,* 2018, **32,** e4364.

11. C. Elamathi, R.J. Butcher and R. Prabhakaran, Anomalous coordination behaviour of 6-methyl-2-oxo-1,2-dihydroquinoline-3-carboxaldehyde-4(*N*)-substituted Schiff bases in Cu(II) complexes: Studies of structure, biomolecular interactions and cytotoxicity, *Appl. Organomet. Chem.,* 2019, **33**, e4659.

12. K. Jeyalakshmi, N. Selvakumaran, N.S.P. Bhuvanesh, A. Sreekanth and R. Karvembu, DNA/protein binding and cytotoxicity studies of copper(II) complexes containing N, N′, N″-trisubstituted guanidine ligands*, RSC Adv.,* 2014, **4**, 17179.

13. C. Kontogiorgis and D.H. Litina, *J. Enzyme Inhib. Med. Chem.,* 2003, **18**, 63.

14. Z.C. Liu, B.D. Wang, B. Li, Q. Wang, Z.Y. Yang, T.R. Li and Y. Li, *Eur. J. Med. Chem.,* 2010, **45**, 5353-5361.

15. M. Safavi, A. Foroumadi, M. Nakhjiri, M. Abdollahi, A. Shafiee, H. Ilkhani, M.R. Ganjali, S.H. Hosseinimehr and S. Emami, *Bioorg. Med. Chem. Lett.,* 2010, **20**, 3070–3073.

16. E. Turkkan, U. Sayin, E. Erbilen, S. Pehlivanoglu, G. Erdogan, H.U. Tasdemir, A.Q. Saf, L. Guler and A.G. Akgemci, *J. Organomet. Chem.,* 2017, **831**, 23-35.